Exploring the remnant properties of precessing black hole binaries by combining numerical relativity and extreme mass ratio (EMRI) data sets

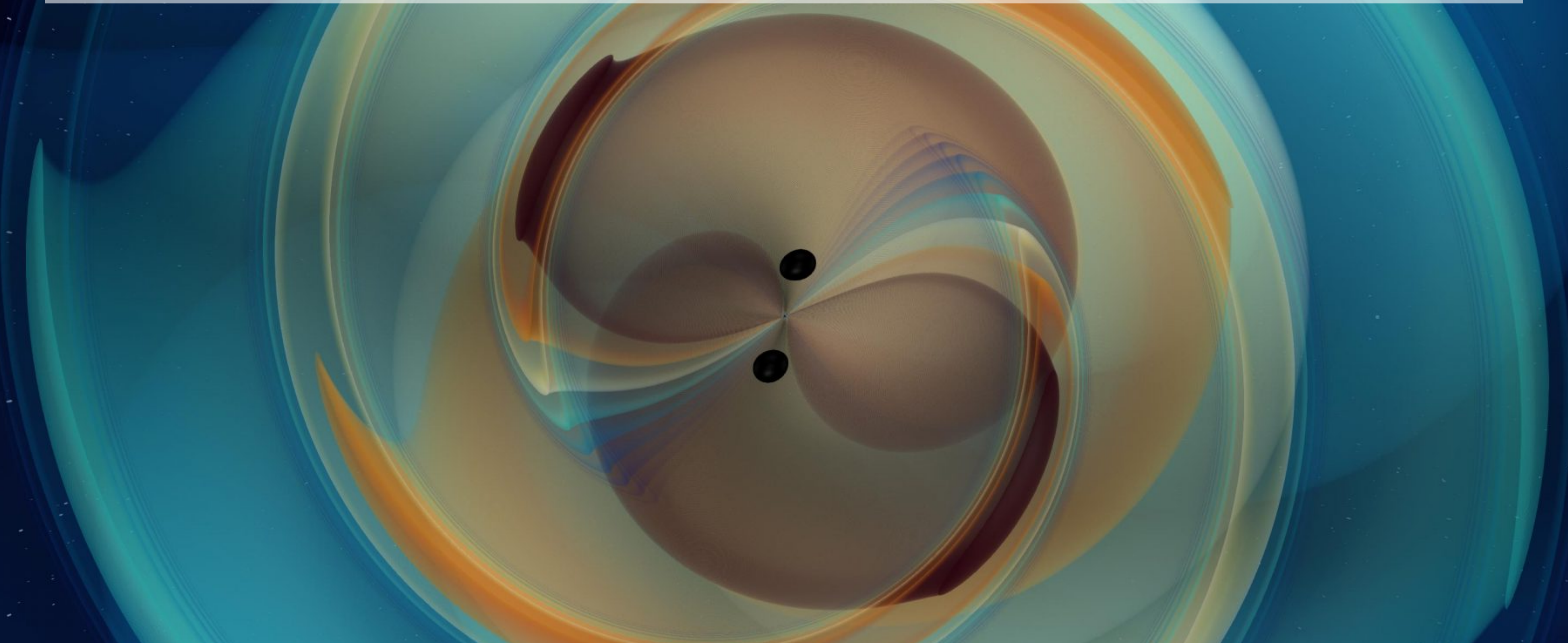

Maria de Lluc Planas (m.planas@uib.es, Universitat de les Illes Balears)

SUPERVISOR: Dr. Sascha Husa

Universitat de les Illes Balears | IAC3 Institute of Applied Computing & Community Code.

CAPRA 02-07 July 2023

Exploring the remnant properties of precessing black hole binaries by combining numerical relativity and extreme mass ratio (EMRI) data sets

We thank Scott A. Hughes, Anuj Apte, Gaurav Khanna and Halston Lim for providing the EMRI waveforms used in this project.

I also extend my sincere appreciation to the CAPRA organising committee, the EDI team and the NBI for their financial support.

Maria de Lluc Planas (m.planas@uib.es, **Universitat de les Illes Balears**)

Supervisor: Dr. Sascha Husa

CAPRA 02-07 July 2023

Gravitational Waves from Black Hole Binaries

- **Black hole binaries** (BBH) are the most detected **source** of gravitational waves (GWs).
- The parameter space to model BBHs is 7-**dimensional** for circular orbits $(q, \overrightarrow{\chi_1}, \overrightarrow{\chi_2})$:
  - **Kerr black holes:** $0 \leq \chi = \dfrac{cJ}{GM^2} \leq 1$.
  - $q = \dfrac{m_1}{m_2} \geq 1$, $\eta = \dfrac{q}{(q+1)^2}$.

Gravitational Waves from Black Hole Binaries

- **Black hole binaries** (BBH) are the most detected **source** of gravitational waves (GWs).
- The parameter space to model BBHs is **7-dimensional** for circular orbits $(q, \overrightarrow{\chi_1}, \overrightarrow{\chi_2})$:
  - **Kerr black holes:** $0 \leq \chi = \dfrac{cJ}{GM^2} \leq 1$.
  - $q = \dfrac{m_1}{m_2} \geq 1$, $\eta = \dfrac{q}{(q+1)^2}$.

Combine different sources of information to UNDERSTAND the full precessing parameter space.

Gravitational Waves from Black Hole Binaries

- **Black hole binaries** (BBH) are the most detected **source** of gravitational waves (GWs).
- The parameter space to model BBHs is 7-**dimensional** for circular orbits $(q, \overrightarrow{\chi_1}, \overrightarrow{\chi_2})$:
  - **Kerr black holes:** $0 \leq \chi = \dfrac{cJ}{GM^2} \leq 1$.
  - $q = \dfrac{m_1}{m_2} \geq 1$, $\eta = \dfrac{q}{(q+1)^2}$.

Combine different sources of information to UNDERSTAND the full precessing parameter space.

Dynamical Evolution

$$\vec{J}(t) = \overrightarrow{L}(t) + \vec{S}(t) = \overrightarrow{L}(t) + m_1^2\overrightarrow{\chi_1}(t) + m_2^2\overrightarrow{\chi_2}(t)\,.$$

- **Black hole binaries** (BBH) are the most detected **source** of gravitational waves (GWs).
- The parameter space to model BBHs is 7-**dimensional** for circular orbits $(q, \overrightarrow{\chi_1}, \overrightarrow{\chi_2})$:
  - **Kerr black holes:** $0 \leq \chi = \dfrac{cJ}{GM^2} \leq 1$.
  - $q = \dfrac{m_1}{m_2} \geq 1$, $\eta = \dfrac{q}{(q+1)^2}$.

Combine different sources of information to UNDERSTAND the full precessing parameter space.

DYNAMICAL EVOLUTION

$$\vec{J}(t) = \overrightarrow{L}(t) + \vec{S}(t) = \overrightarrow{L}(t) + m_1^2 \overrightarrow{\chi_1}(t) + m_2^2 \overrightarrow{\chi_2}(t)\,.$$

ALIGNED-SPIN SYSTEMS: $\overrightarrow{L} \parallel \vec{S}$

timescales: orbital (E_{rad})>radial

(q, χ_1^L, χ_2^L): 3-dim

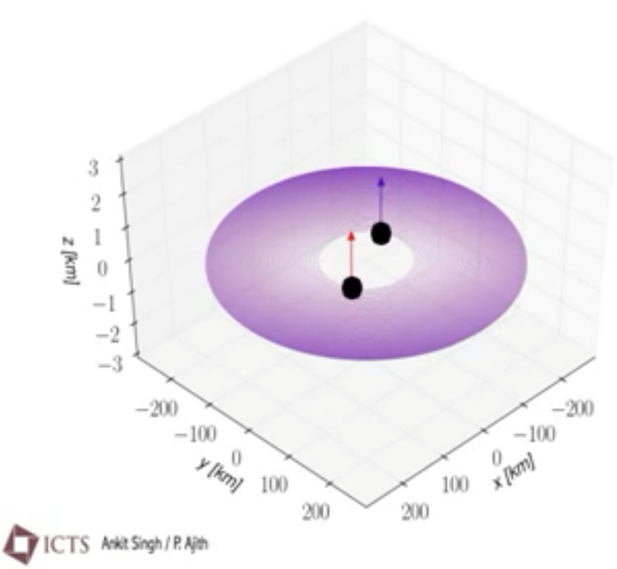

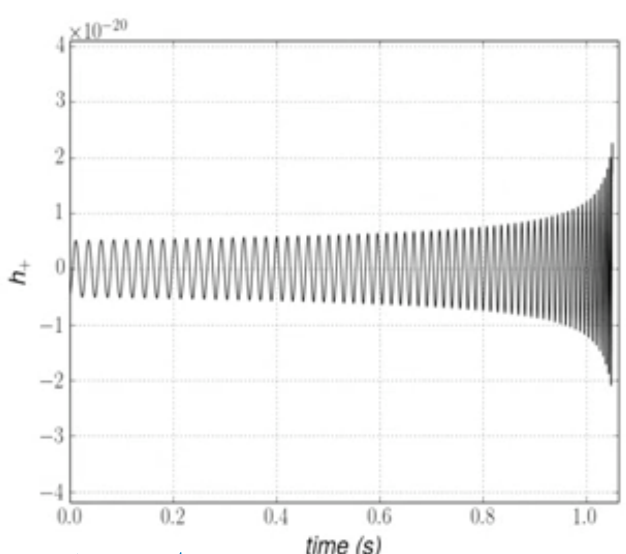

Credit: Ankit Singh/ P. Ajith/ ICTS

- **Black hole binaries** (BBH) are the most detected **source** of gravitational waves (GWs).
- The parameter space to model BBHs is 7-**dimensional** for circular orbits $(q, \overrightarrow{\chi_1}, \overrightarrow{\chi_2})$:
  - **Kerr black holes:** $0 \leq \chi = \dfrac{cJ}{GM^2} \leq 1$.
  - $q = \dfrac{m_1}{m_2} \geq 1$, $\eta = \dfrac{q}{(q+1)^2}$.

Combine different sources of information to UNDERSTAND the full precessing parameter space.

DYNAMICAL EVOLUTION

$$\vec{J}(t) = \overrightarrow{L}(t) + \vec{S}(t) = \overrightarrow{L}(t) + m_1^2\overrightarrow{\chi_1}(t) + m_2^2\overrightarrow{\chi_2}(t)\,.$$

ALIGNED-SPIN SYSTEMS: $\overrightarrow{L} \parallel \vec{S}$

timescales: orbital ($E_{\rm rad}$)>radial

(q, χ_1^L, χ_2^L): 3-dim

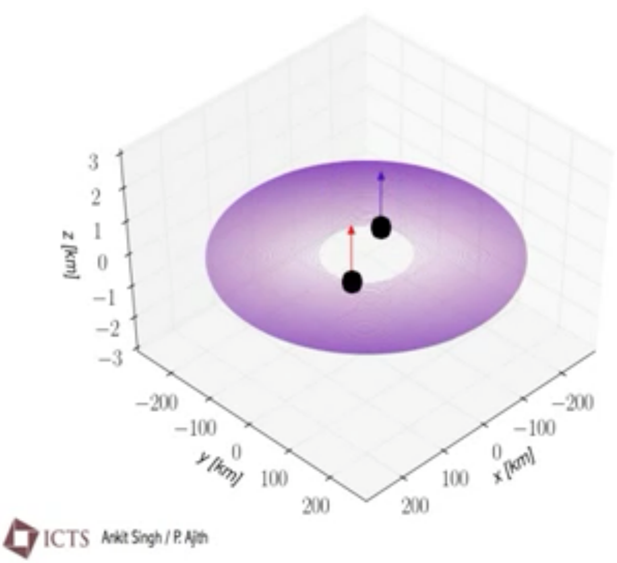

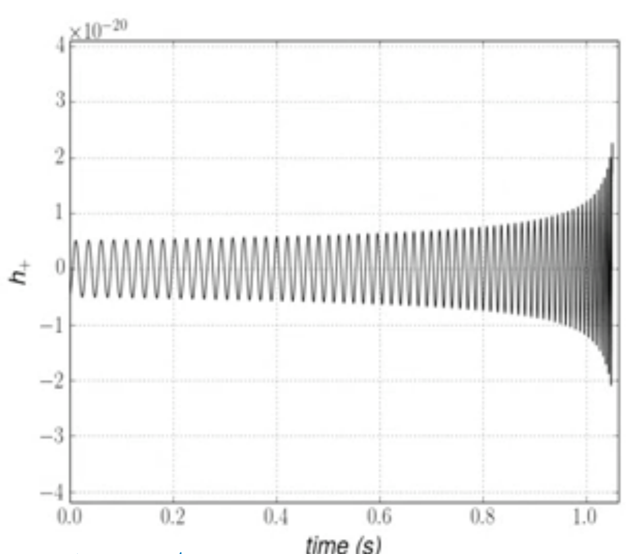

Credit: Ankit Singh/ P. Ajith/ ICTS

PRECESSING SYSTEMS: $\overrightarrow{L} \nparallel \vec{S}$

timescales: orbital ($E_{\rm rad}$)>precessing (P)>radial

$(q, \overrightarrow{\chi_1}, \overrightarrow{\chi_2})$: 7-dim

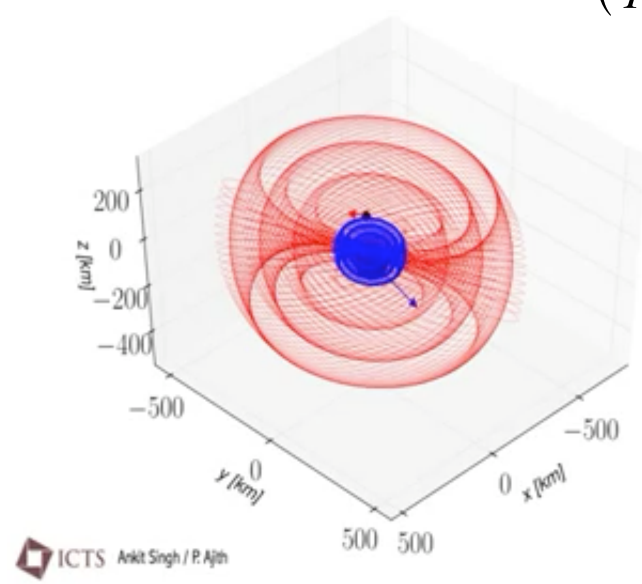

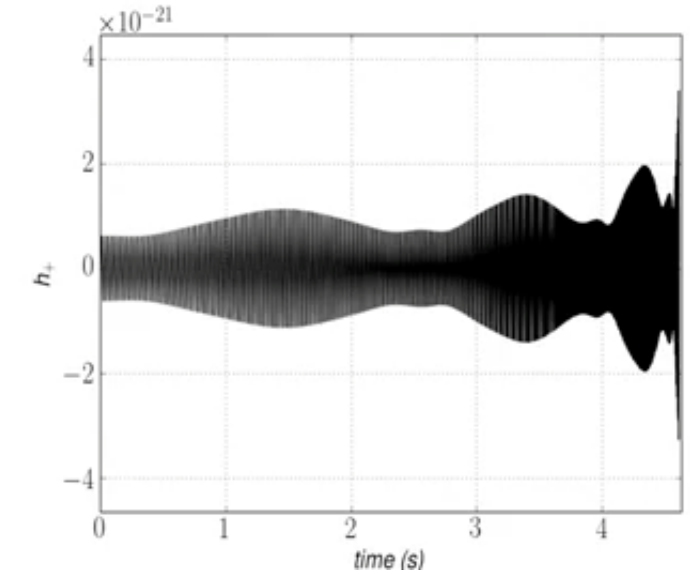

Credit: Ankit Singh/ P. Ajith/ ICTS

Precessing Binary Systems: Introduction

Precessing Systems present two particular difficulties: 7-dim space + no symmetries.

Precessing Systems present two particular difficulties:

- 7-DIMENSIONAL SPACE: **too large** to cover with **NR** simulations.

Available NR data sets (**Fig. 1**):

- SXS [Boyle, M. et al. (2019)]: 1400 sims ($q \leq 6$).
- BAM [Hamilton, E. et al. (2023)]: 80 sims ($q \leq 8, |\chi_2| = 0$).
- Einstein Toolkit [Husa, S. et al. (in prep)]: 15 sims ($4 \leq q \leq 18$).

Black hole perturbation theory (BHPT):

- EMRI [Apte, A. et al., Lim, H. et al. (2019)]: 5925 sims ($q = 1000$, $S_2 \approx 0$).

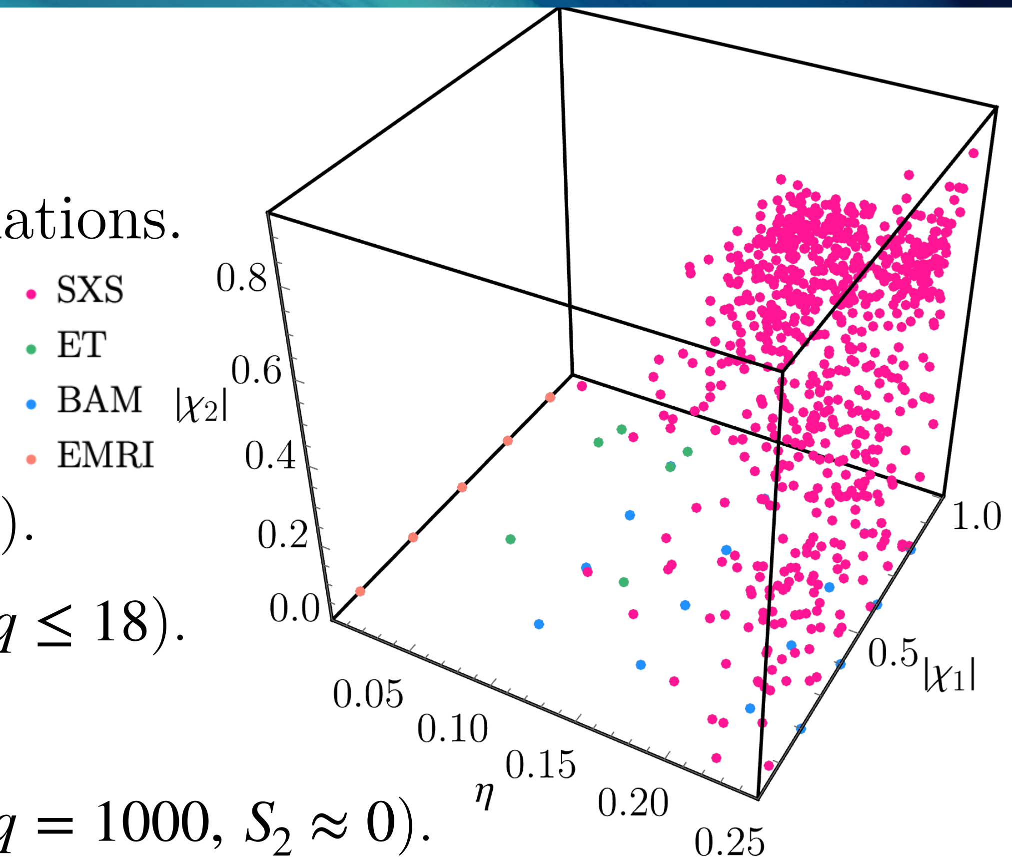

Figure 1: Available precessing data sets.

Precessing Binary Systems: Introduction

Precessing Systems present two particular difficulties:

- 7-DIMENSIONAL SPACE: **too large** to cover with **NR** simulations.

  Available NR data sets (**Fig. 1**):

  - SXS [Boyle, M. et al. (2019)]: 1400 sims ($q \leq 6$).
  - BAM [Hamilton, E. et al. (2023)]: 80 sims ($q \leq 8, |\chi_2| = 0$).
  - Einstein Toolkit [Husa, S. et al. (in prep)]: 15 sims ($4 \leq q \leq 18$).

  Black hole perturbation theory (BHPT):

  - EMRI [Apte, A. et al., Lim, H. et al. (2019)]: 5925 sims ($q = 1000$, $S_2 \approx 0$).

  More data:

  - `NRSur7dq4` [Varma, V. (2019)]: NR calibrated model ($q \leq 4$).

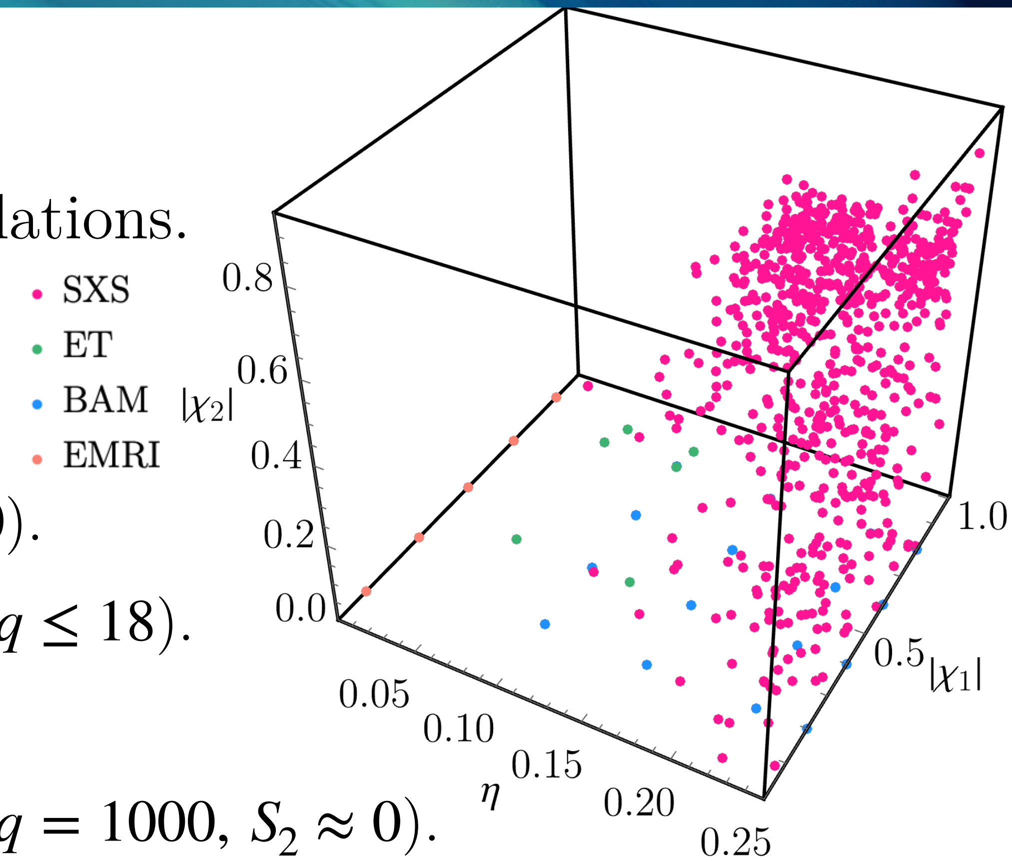

Figure 1: Available precessing data sets.

PRECESSING SYSTEMS present two particular difficulties:

- 7-DIMENSIONAL SPACE: **too large** to cover with **NR** simulations.

  Available NR data sets (**FIG. 1**):

  - SXS [Boyle, M. et al. (2019)]: 1400 sims ($q \leq 6$).
  - BAM [Hamilton, E. et al. (2023)]: 80 sims ($q \leq 8, |\chi_2| = 0$).
  - Einstein Toolkit [Husa, S. et al. (in prep)]: 15 sims ($4 \leq q \leq 18$).

  Black hole perturbation theory (BHPT):

  - EMRI [Apte, A. et al., Lim, H. et al. (2019)]: 5925 sims ($q = 1000$, $S_2 \approx 0$).

  More data:

  - `NRSur7dq4` [Varma, V. (2019)]: NR calibrated model ($q \leq 4$).

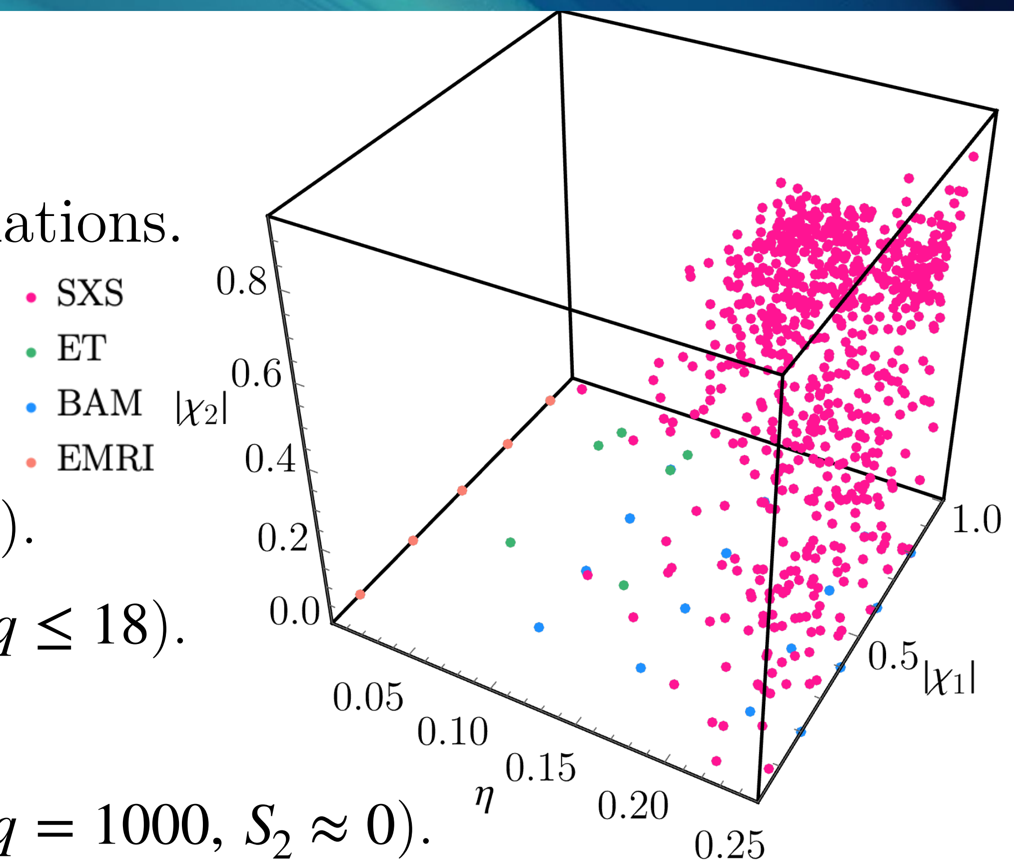

Figure 1: Available precessing data sets.

- PRECESSING MOTION of $\overrightarrow{L}$ and $\overrightarrow{S_i}$: **NO** natural **inertial frame**.

  $\overrightarrow{L}(t)$ and $\overrightarrow{\chi_i}(t)$ precess around an inertial frame defined at a t_{ref}:

  - **$\hat{z}-$AXIS:** $\overrightarrow{L}(t_{\text{ref}})$ (L-FRAME).
  - **$\hat{x}-$AXIS:** $\overrightarrow{r_1}(t_{\text{ref}}) - \overrightarrow{r_2}(t_{\text{ref}})$.

$$\boxed{\hat{z} = \hat{\omega}(-100M) = \frac{\vec{r} \times \vec{v}}{r^2}}$$

Consistent dataset

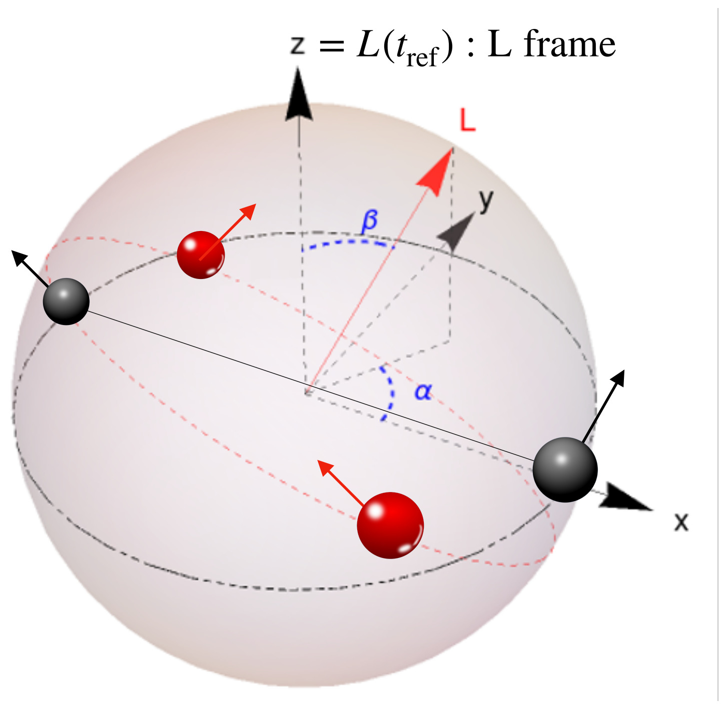

Figure 2: Inertial frames definitions.

PRECESSING SYSTEMS present two particular difficulties:

- 7-DIMENSIONAL SPACE: **too large** to cover with **NR** simulations.

  Available NR data sets (**FIG. 1**):

  - SXS [Boyle, M. et al. (2019)]: 1400 sims ($q \leq 6$).
  - BAM [Hamilton, E. et al. (2023)]: 80 sims ($q \leq 8, |\chi_2| = 0$).
  - Einstein Toolkit [Husa, S. et al. (in prep)]: 15 sims ($4 \leq q \leq 18$).

  Black hole perturbation theory (BHPT):

  - EMRI [Apte, A. et al., Lim, H. et al. (2019)]: 5925 sims ($q = 1000$, $S_2 \approx 0$).

  More data:

  - `NRSur7dq4` [Varma, V. (2019)]: NR calibrated model ($q \leq 4$).

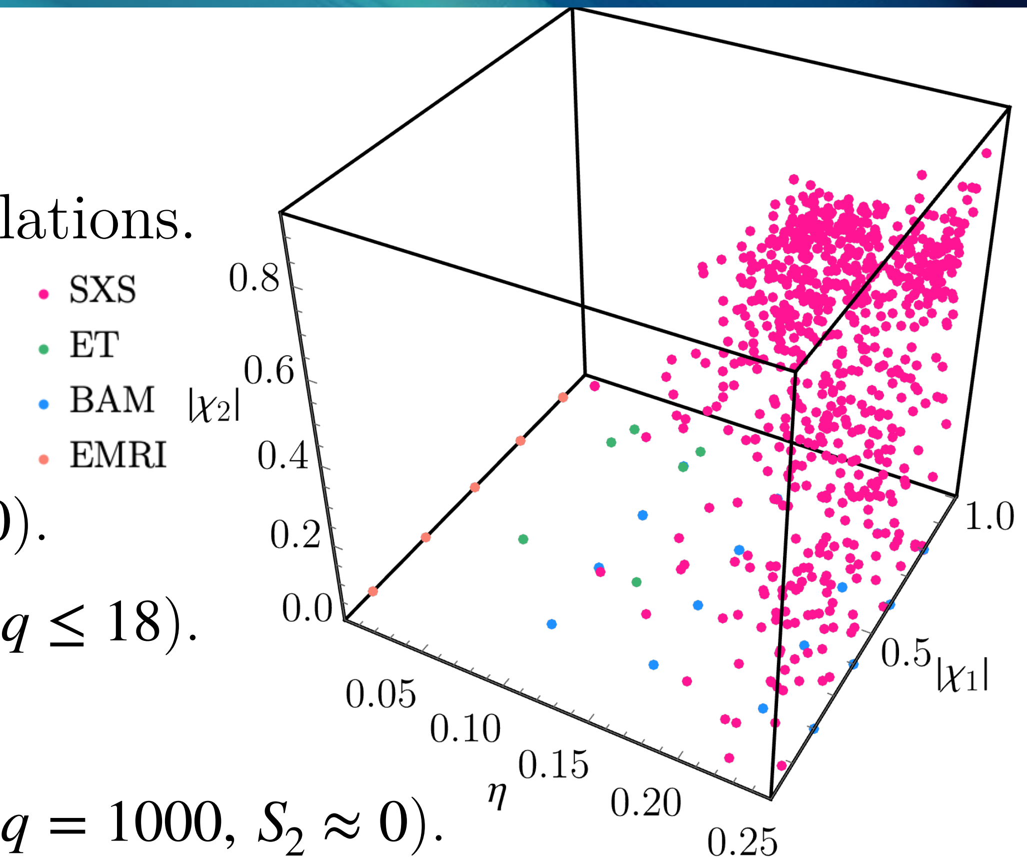

Figure 1: Available precessing data sets.

- PRECESSING MOTION of $\vec{L}$ and $\vec{S_i}$: **NO** natural **inertial frame**.

  $\vec{L}(t)$ and $\vec{\chi_i}(t)$ precess around an inertial frame defined at a t_{ref}:

  - **$\hat{z}$−AXIS:** $\vec{L}(t_{\text{ref}})$ (L-FRAME).
  - **$\hat{x}$−AXIS:** $\vec{r_1}(t_{\text{ref}}) - \vec{r_2}(t_{\text{ref}})$.

$$\boxed{\hat{z} = \hat{\omega}(-100M) = \frac{\vec{r} \times \vec{v}}{r^2}}$$

Consistent dataset

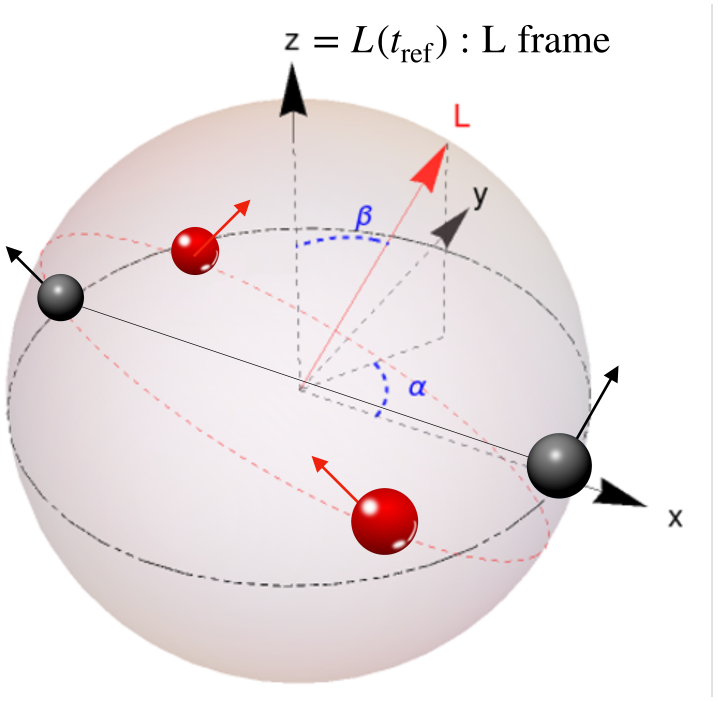

Figure 2: Inertial frames definitions.

More work needs to be done for EMRIs...

Dataset Generation: EMRIs

5925 EMRIs [Apte, A. et al., Lim, H. et al. (2019)] ($M/\mu = 1000$, varying a, I and θ_f, see **Fig. 3**) including TRAJECTORIES, CONSTANTS OF MOTION and WAVEFORMS.

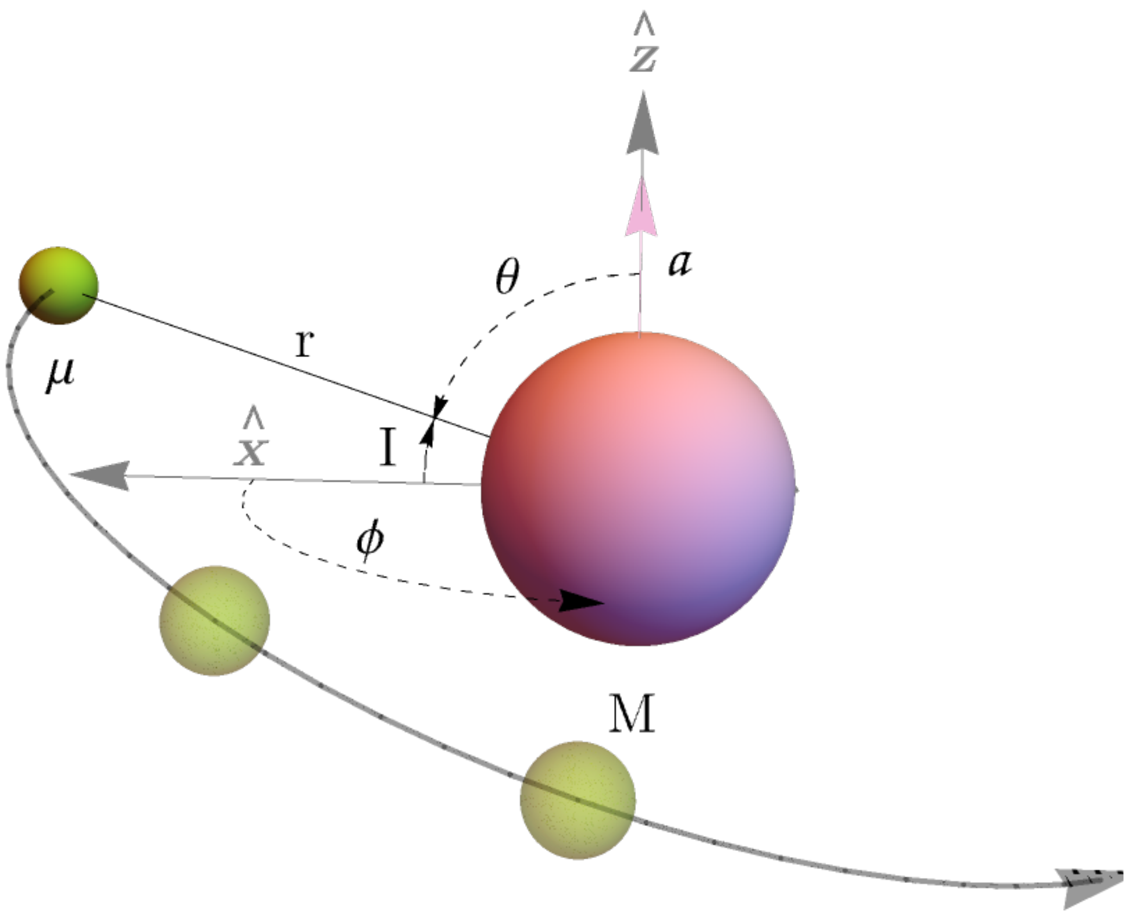

5925 EMRIs [Apte, A. et al., Lim, H. et al. (2019)] ($M/\mu = 1000$, varying a, I and θ_f, see **Fig. 3**) including TRAJECTORIES, CONSTANTS OF MOTION and WAVEFORMS.

1. **Reparametrization** of the orbital parameters in terms of LIGO conventions.

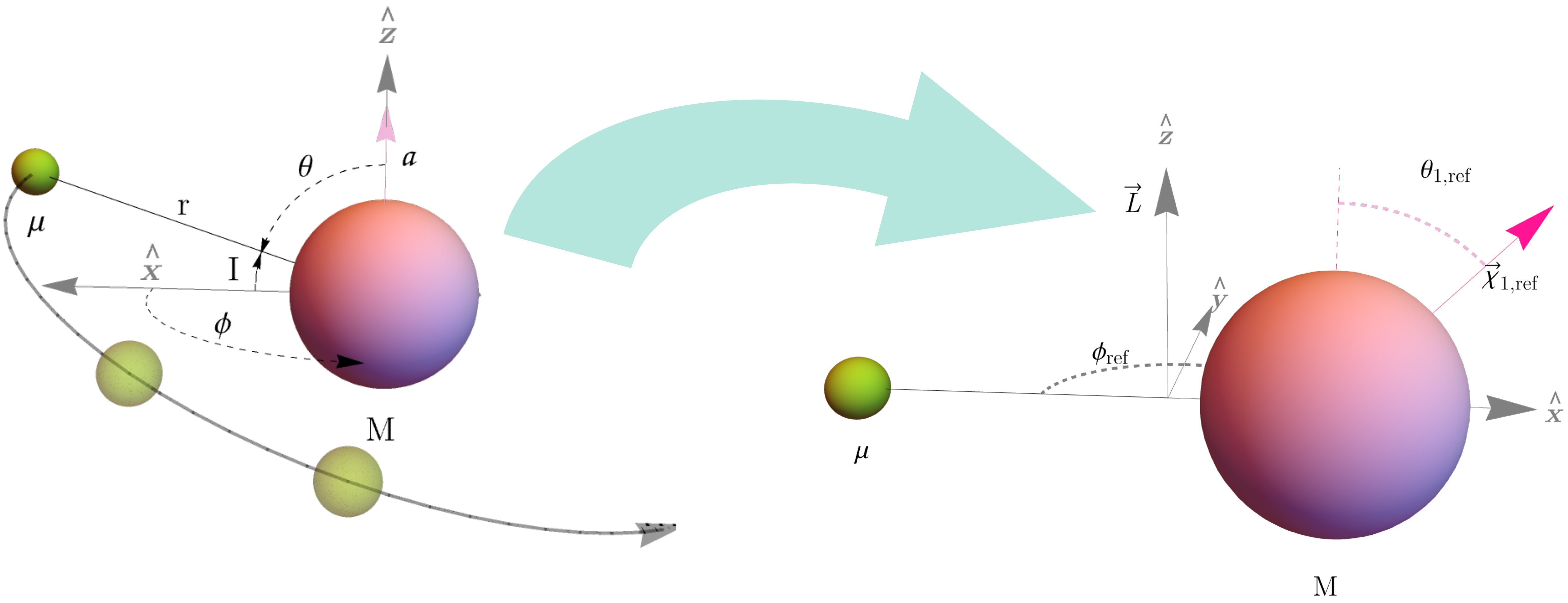

Dataset Generation: EMRIs

5925 EMRIs [Apte, A. et al., Lim, H. et al. (2019)] ($M/\mu = 1000$, varying a, I and θ_f, see **Fig. 3**) including TRAJECTORIES, CONSTANTS OF MOTION and WAVEFORMS.

1. **Reparametrization** of the orbital parameters in terms of LIGO conventions.
2. Computation of the **remnant quantities** $M_f^2 \overrightarrow{\chi_f} = M^2 \vec{a} + \mu M \overrightarrow{L}$ and $M_f = 1 - E_{\mathrm{rad}}$ from the constants of motion E_f, L_z and $Q \approx L_\rho^2$ we get from
   - A. EMRI data.
   - B. Precessing geodesic equations ($I \approx \theta_{\mathrm{ref}}$) at the ISCO.

Dataset Generation: EMRIs

5925 EMRIs [Apte, A. et al., Lim, H. et al. (2019)] ($M/\mu = 1000$, varying a, I and θ_f, see **Fig. 3**) including TRAJECTORIES, CONSTANTS OF MOTION and WAVEFORMS.

1. **Reparametrization** of the orbital parameters in terms of LIGO conventions.
2. Computation of the **REMNANT QUANTITIES** $M_f^2\overrightarrow{\chi_f} = M^2\vec{a} + \mu M\overrightarrow{L}$ and $M_f = 1 - E_{\text{rad}}$ from the constants of motion E_f, L_z and $Q \approx L_\rho^2$ we get from
   A. EMRI data.
   B. Precessing geodesic equations ($I \approx \theta_{\text{ref}}$) at the ISCO.

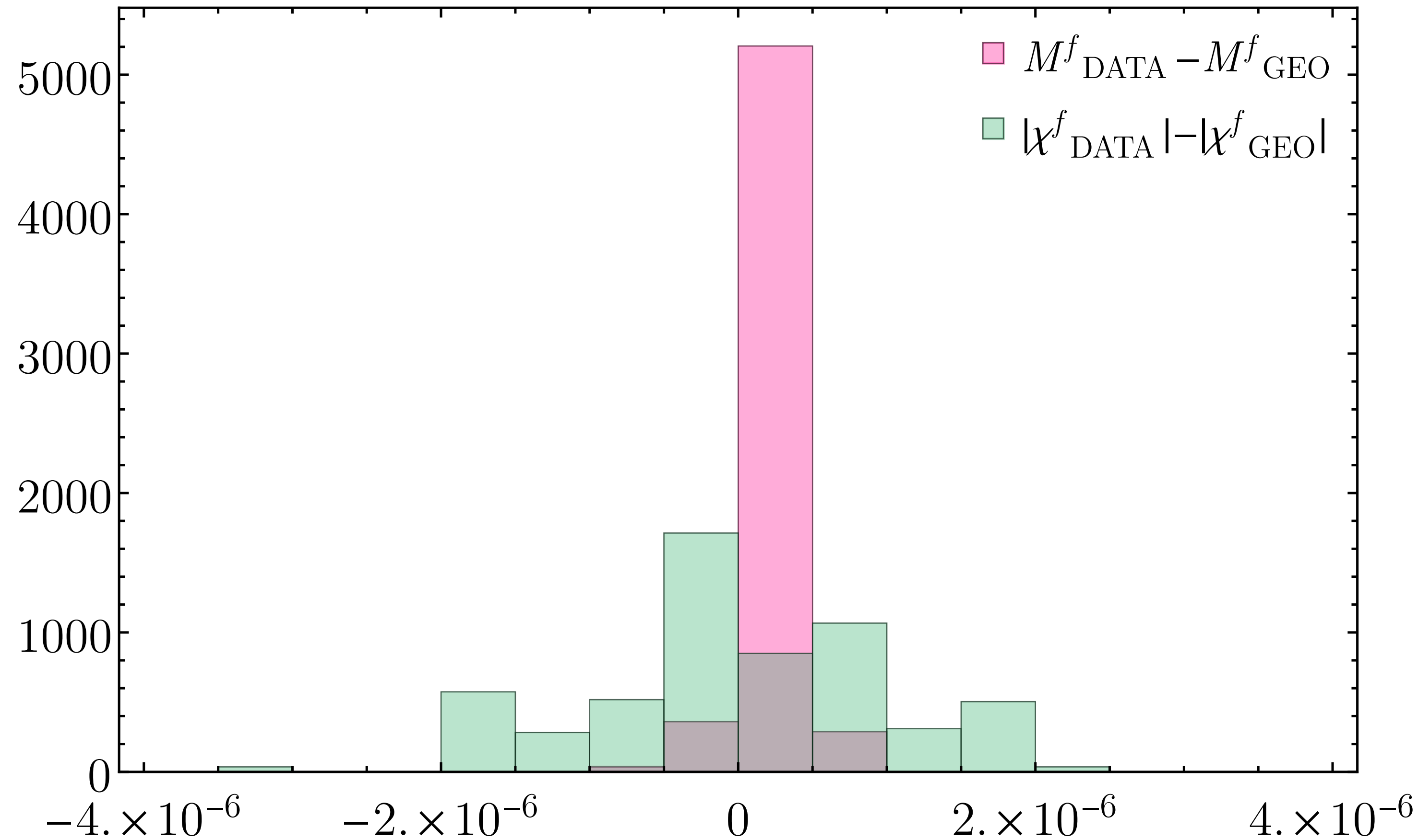

Histogram of the geodesics vs EMRI DIFFERENCES.

Dataset Generation: EMRIs

5925 EMRIs [Apte, A. et al., Lim, H. et al. (2019)] ($M/\mu = 1000$, varying a, I and θ_f, see **Fig. 3**) including TRAJECTORIES, CONSTANTS OF MOTION and WAVEFORMS.

1. **Reparametrization** of the orbital parameters in terms of LIGO conventions.
2. Computation of the **REMNANT QUANTITIES** $M_f^2 \overrightarrow{\chi_f} = M^2 \vec{a} + \mu M \overrightarrow{L}$ and $M_f = 1 - E_{\mathrm{rad}}$ from the constants of motion E_f, L_z and $Q \approx L_\rho^2$ we get from
   A. EMRI data.
   B. Precessing geodesic equations ($I \approx \theta_{\mathrm{ref}}$) at the ISCO.

Use **geodesics** to obtain more data.

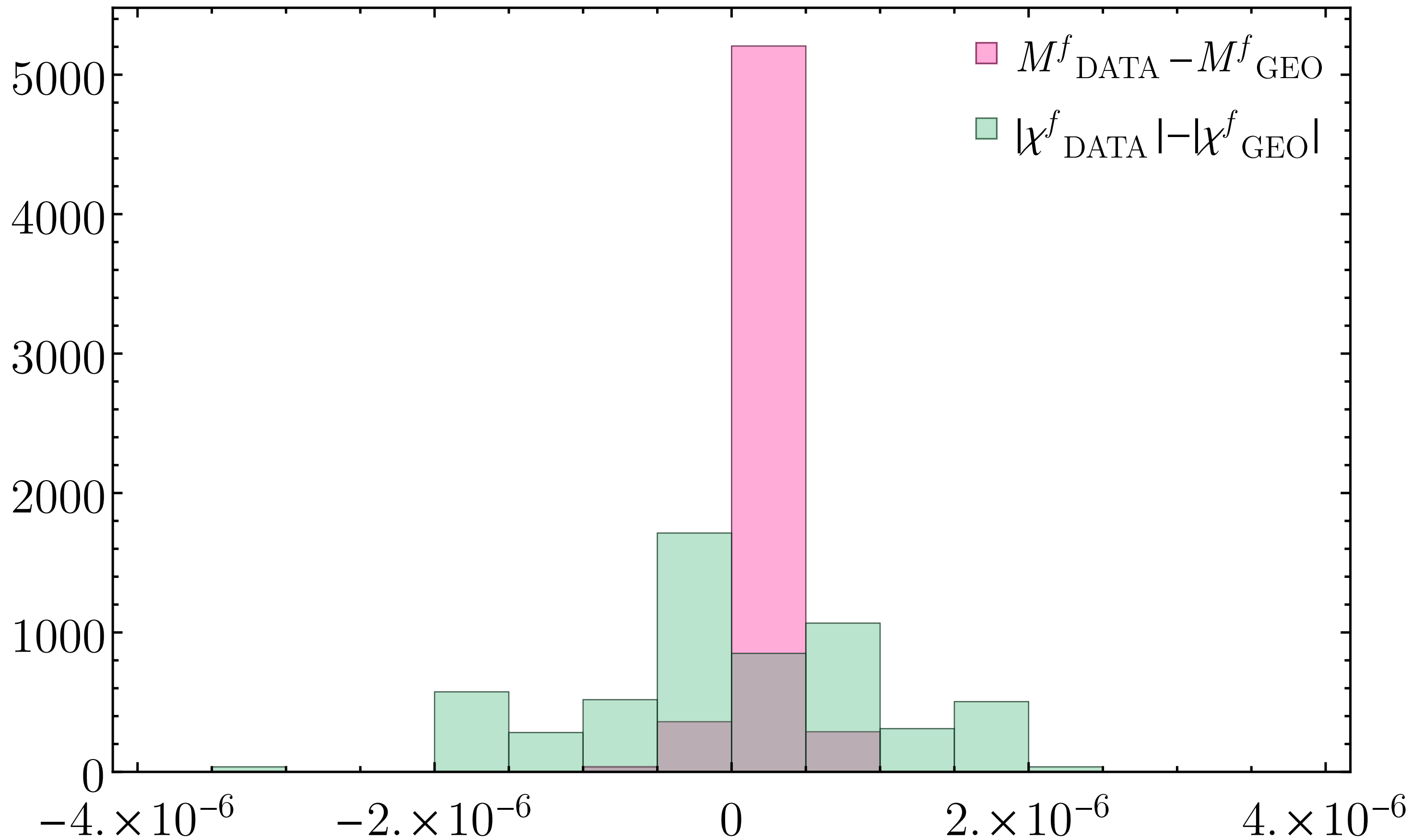

Histogram of the geodesics vs EMRI DIFFERENCES.

Precessing Binary Systems: Dataset Applications

The **Precessing Dataset** can be used to **calibrate** precessing models.

Current Data limitation e.g. `NRSur7dq4` ($q \leq 6$), `PhenomXO4a` (single spin and $q \leq 8$).

Precessing Binary Systems: Dataset Applications

The **Precessing Dataset** can be used to **calibrate** precessing models.

Current Data limitation e.g. `NRSur7dq4` ($q \leq 6$), `PhenomXO4a` (single spin and $q \leq 8$).

Idea

→ **combine** NR data + analytical information.

Precessing Binary Systems: Dataset Applications

The **Precessing Dataset** can be used to **calibrate** precessing models.

Application

Current Data limitation e.g. NRSur7dq4 ($q \leq 6$), PhenomXO4a (single spin and $q \leq 8$).

Idea

→ **combine** NR data + analytical information.

→ **Remnant Model** across all q, $|\chi_1| \leq 0.8$, $|\chi_2| = 0$ using Hierarchical Methods.

Precessing Binary Systems: Dataset Applications

The Precessing Dataset can be used to **calibrate** precessing models.

Application

Current Data limitation e.g. `NRSur7dq4` ($q \leq 6$), `PhenomXO4a` (single spin and $q \leq 8$).

Idea

→ **combine** NR data + analytical information.

→ Remnant Model across all q, $|\chi_1| \leq 0.8$, $|\chi_2| = 0$ using Hierarchical Methods.

What is the Best Quantity to fit for each remnant property?

The **PRECESSING DATASET** can be used to **calibrate** precessing models.

APPLICATION

CURRENT DATA LIMITATION e.g. `NRSur7dq4` ($q \leq 6$), `PhenomXO4a` (single spin and $q \leq 8$).

IDEA

→ **combine** NR data + analytical information.

→ **REMNANT MODEL** across all q, $|\chi_1| \leq 0.8$, $|\chi_2| = 0$ using HIERARCHICAL METHODS.

FINAL MASS

Since $E_{\rm rad}^{\rm AS} \approx E_{\rm rad}^{\rm prec}$, we can generate a **fit** for ΔE:

$$\boxed{\Delta E = E_{\rm rad}^{\rm prec}\left(q, |\chi_1|, \theta_{\vec{\chi_1}, \vec{L}}\right) - E_{\rm rad}^{\rm AS}\left(q, |\chi_1| \cos(\theta_{\vec{\chi_1}, \vec{L}})\right)}$$

$$M_f = 1 - E_{\rm rad} = 1 - \left(E_{\rm rad}^{\rm AS}(q, \chi_1 \cos(\theta)) + \Delta E(q, |\chi_1|, \theta)\right)$$

Precessing Binary Systems: Dataset Applications

The **Precessing Dataset** can be used to **calibrate** precessing models.

Application

Current Data limitation e.g. NRSur7dq4 ($q \leq 6$), PhenomXO4a (single spin and $q \leq 8$).

Idea

combine NR data + analytical information.

Remnant Model across all q, $|\chi_1| \leq 0.8$, $|\chi_2| = 0$ using Hierarchical Methods.

Final Mass

Since $E_{\text{rad}}^{\text{AS}} \approx E_{\text{rad}}^{\text{prec}}$, we can generate a **fit** for ΔE:

$$\boxed{\Delta E = E_{\text{rad}}^{\text{prec}}\left(q, |\chi_1|, \theta_{\vec{\chi_1},\vec{L}}\right) - E_{\text{rad}}^{\text{AS}}\left(q, |\chi_1|\cos(\theta_{\vec{\chi_1},\vec{L}})\right)}$$

$$M_f = 1 - E_{\text{rad}} = 1 - \left(E_{\text{rad}}^{\text{AS}}(q, \chi_1\cos(\theta)) + \Delta E(q, |\chi_1|, \theta)\right)$$

Final Spin Magnitude

Assuming a correction to PhenomXPHM

$$\boxed{|\chi_f^{\text{prec}}| = \sqrt{|\chi_f^{\text{AS}}|^2 + \frac{m_1^4}{M_f^4}{\chi_1^{\perp}}^2 + \delta^2}\,.}$$

Where:

- $|\chi_f^{\text{AS}}| = \text{PhenomX}_{\text{fit}}$.
- $M_f = 1 - E_{\text{rad}}^{\text{prec}} \approx 1 - E_{\text{rad}}^{\text{AS}}$.
- We **fit** $\delta^2(q, |\chi_1|, \theta_{\vec{\chi_1},\vec{L}})$,

PRECESSING BINARY SYSTEMS: DATASET APPLICATIONS

The **PRECESSING DATASET** can be used to **calibrate** precessing models.

APPLICATION

CURRENT DATA LIMITATION e.g. `NRSur7dq4` ($q \leq 6$), `PhenomXO4a` (single spin and $q \leq 8$).

IDEA → **combine** NR data + analytical information.

→ **REMNANT MODEL** across all q, $|\chi_1| \leq 0.8$, $|\chi_2| = 0$ using HIERARCHICAL METHODS.

FINAL MASS

Since $E_{\rm rad}^{\rm AS} \approx E_{\rm rad}^{\rm prec}$, we can generate a **fit** for ΔE:

$$\boxed{\Delta E = E_{\rm rad}^{\rm prec}\left(q, |\chi_1|, \theta_{\vec{\chi}_1,\vec{L}}\right) - E_{\rm rad}^{\rm AS}\left(q, |\chi_1|\cos(\theta_{\vec{\chi}_1,\vec{L}})\right)}$$

$$\downarrow$$

$$M_f = 1 - E_{\rm rad} = 1 - \left(E_{\rm rad}^{\rm AS}(q, \chi_1\cos(\theta)) + \Delta E(q, |\chi_1|, \theta)\right)$$

FINAL SPIN MAGNITUDE

Assuming a correction to `PhenomXPHM`

$$\boxed{|\chi_f^{\rm prec}| = \sqrt{|\chi_f^{\rm AS}|^2 + \frac{m_1^4}{M_f^4}{\chi_1^{\perp}}^2 + \delta^2}\,.}$$

Where:

- $|\chi_f^{\rm AS}| = \text{PhenomX}_{\rm fit}$.
- $M_f = 1 - E_{\rm rad}^{\rm prec} \approx 1 - E_{\rm rad}^{\rm AS}$.
- We **fit** $\delta^2(q, |\chi_1|, \theta_{\vec{\chi}_1,\vec{L}})$,

Precessing Binary Systems: Dataset Applications

The **Precessing Dataset** can be used to **calibrate** precessing models.

Application

Current Data limitation e.g. NRSur7dq4 ($q \leq 6$), PhenomXO4a (single spin and $q \leq 8$).

Idea → **combine** NR data + analytical information.

→ **Remnant Model** across all q, $|\chi_1| \leq 0.8$, $|\chi_2| = 0$ using Hierarchical Methods.

Final Mass

Since $E_{\rm rad}^{\rm AS} \approx E_{\rm rad}^{\rm prec}$, we can generate a **fit** for $\boldsymbol{\Delta E}$:

$$\boxed{\Delta E = E_{\rm rad}^{\rm prec}\left(q, |\chi_1|, \theta_{\vec{\chi}_1,\vec{L}}\right) - E_{\rm rad}^{\rm AS}\left(q, |\chi_1|\cos(\theta_{\vec{\chi}_1,\vec{L}})\right)}$$

$$M_f = 1 - E_{\rm rad} = 1 - \left(E_{\rm rad}^{\rm AS}(q, \chi_1\cos(\theta)) + \Delta E(q, |\chi_1|, \theta)\right)$$

Final Spin Magnitude

Assuming a correction to PhenomXPHM

$$\boxed{|\chi_f^{\rm prec}| = \sqrt{|\chi_f^{\rm AS}|^2 + \frac{m_1^4}{M_f^4}{\chi_1^{\perp}}^2 + \delta^2}\,.}$$

Where:

- $|\chi_f^{\rm AS}| = \mathrm{PhenomX}_{\rm fit}$.
- $M_f = 1 - E_{\rm rad}^{\rm prec} \approx 1 - E_{\rm rad}^{\rm AS}$.
- We **fit** $\delta^2(q, |\chi_1|, \theta_{\vec{\chi}_1,\vec{L}})$,

PRECESSING BINARY SYSTEMS: DATASET APPLICATIONS

The **PRECESSING DATASET** can be used to **calibrate** precessing models.

APPLICATION

CURRENT DATA LIMITATION e.g. `NRSur7dq4` ($q \leq 6$), `PhenomXO4a` (single spin and $q \leq 8$).

IDEA

→ **combine** NR data + analytical information.

→ **REMNANT MODEL** across all q, $|\chi_1| \leq 0.8$, $|\chi_2| = 0$ using HIERARCHICAL METHODS.

FINAL MASS

Since $E_{\rm rad}^{\rm AS} \approx E_{\rm rad}^{\rm prec}$, we can generate a **fit** for ΔE:

$$\boxed{\Delta E = E_{\rm rad}^{\rm prec}\left(q, |\chi_1|, \theta_{\vec{\chi_1},\vec{L}}\right) - E_{\rm rad}^{\rm AS}\left(q, |\chi_1| \cos(\theta_{\vec{\chi_1},\vec{L}})\right)}$$

$$M_f = 1 - E_{\rm rad} = 1 - \left(E_{\rm rad}^{\rm AS}(q, \chi_1 \cos(\theta)) + \Delta E(q, |\chi_1|, \theta)\right)$$

FINAL SPIN MAGNITUDE

Assuming a correction to PhenomXPHM

$$\boxed{|\chi_f^{\rm prec}| = \sqrt{|\chi_f^{\rm AS}|^2 + \frac{m_1^4}{M_f^4}{\chi_1^{\perp}}^2 + \delta^2}.}$$

Where:

- $|\chi_f^{\rm AS}| = \text{PhenomX}_{\rm fit}$.
- $M_f = 1 - E_{\rm rad}^{\rm prec} \approx 1 - E_{\rm rad}^{\rm AS}$.
- We **fit** $\delta^2(q, |\chi_1|, \theta_{\vec{\chi_1},\vec{L}})$,

EMRI LIMIT: δ^2 can be obtained **analytically**.

$$|\chi_f^{\text{prec}}| = \sqrt{|\chi_f^{\text{AS}}|^2 + \frac{m_1^4}{M_f^4}{\chi_1^{\perp}}^2 + \delta^2} \rightarrow \boxed{\delta^2 = \frac{m_1^4}{M_f^4}\left[\frac{1}{q^2}(L_z^2 + Q - L_z^{\parallel}) + 2\frac{1}{q}a\cos(I)\left(\sqrt{L_z^2 + Q} - L_z^{\parallel}\right)\right]}$$

EMRI Limit: δ^2 can be obtained **analytically**.

$$|\chi_f^{\rm prec}| = \sqrt{|\chi_f^{\rm AS}|^2 + \frac{m_1^4}{M_f^4}\chi_1^{\perp 2} + \delta^2} \rightarrow \boxed{\delta^2 = \frac{m_1^4}{M_f^4}\left[\frac{1}{q^2}(L_z^2 + Q - L_z^{\parallel}) + 2\frac{1}{q}a\cos(I)\left(\sqrt{L_z^2+Q} - L_z^{\parallel}\right)\right]}$$

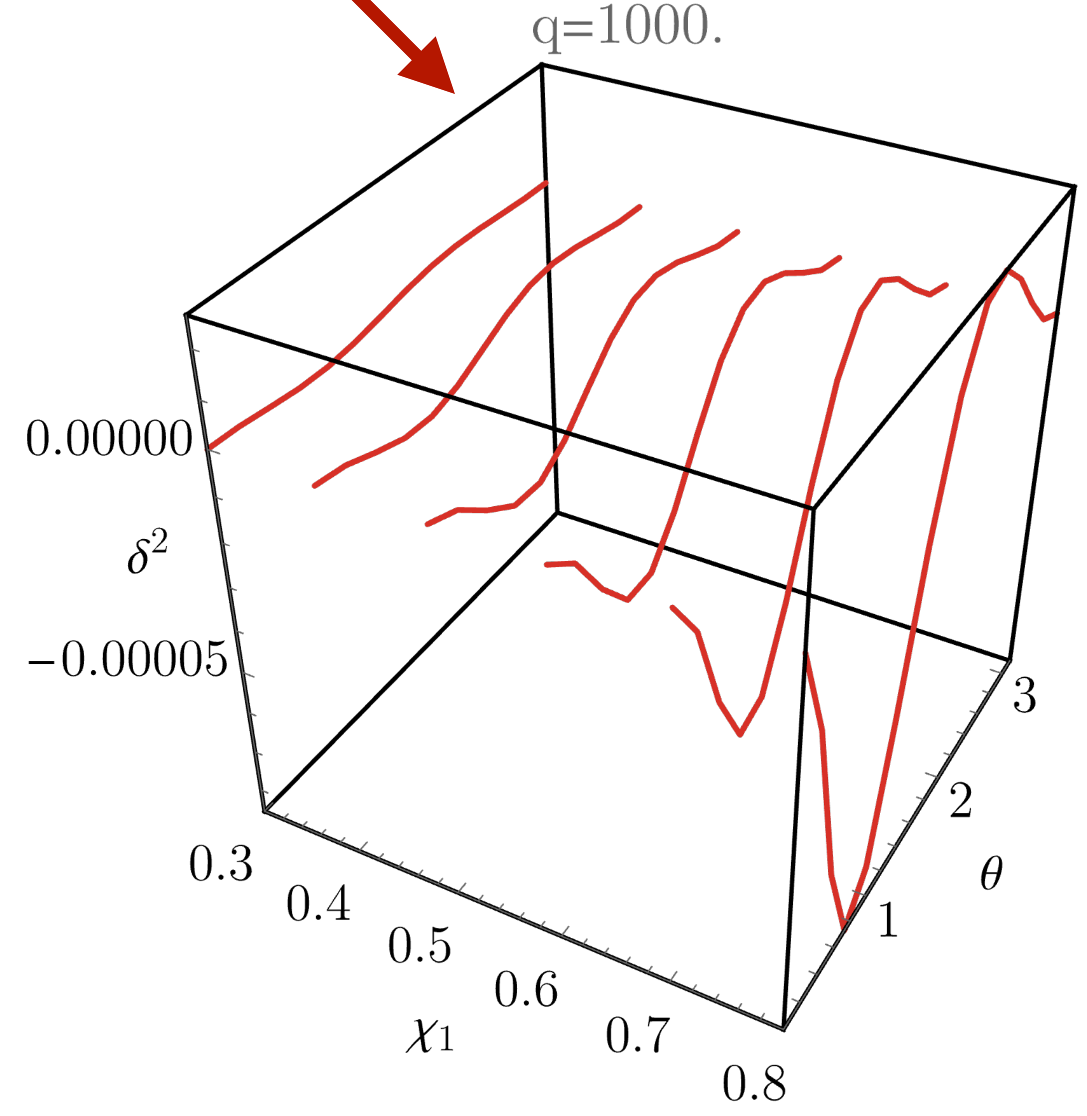

EMRI Limit: δ^2 can be obtained **analytically**.

$$|\chi_f^{\text{prec}}| = \sqrt{|\chi_f^{\text{AS}}|^2 + \frac{m_1^4}{M_f^4}\chi_1^{\perp 2} + \delta^2} \rightarrow \boxed{\delta^2 = \frac{m_1^4}{M_f^4}\left[\frac{1}{q^2}(L_z^2 + Q - L_z^{\parallel}) + 2\frac{1}{q}a\cos(I)\left(\sqrt{L_z^2+Q} - L_z^{\parallel}\right)\right]}$$

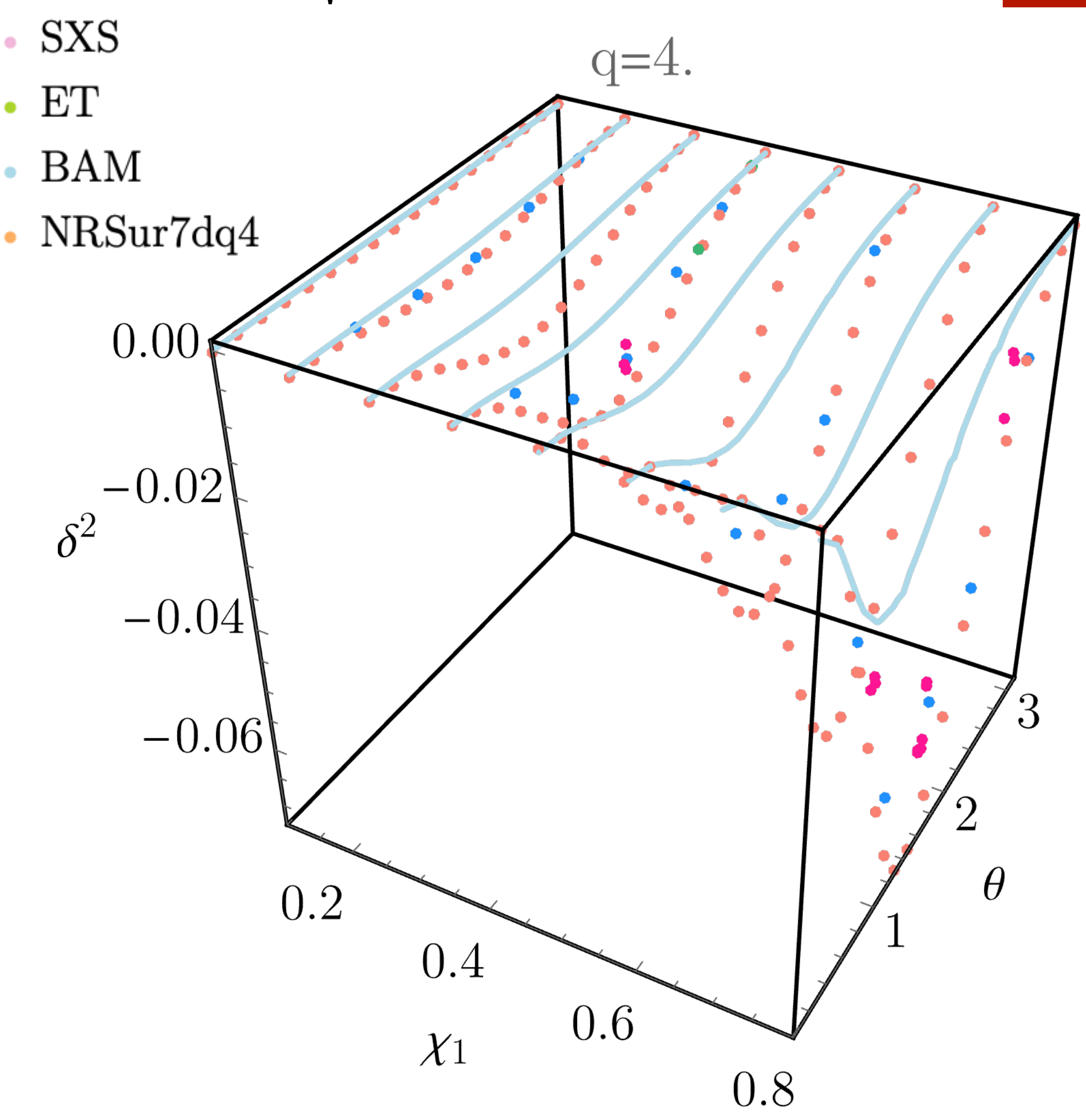

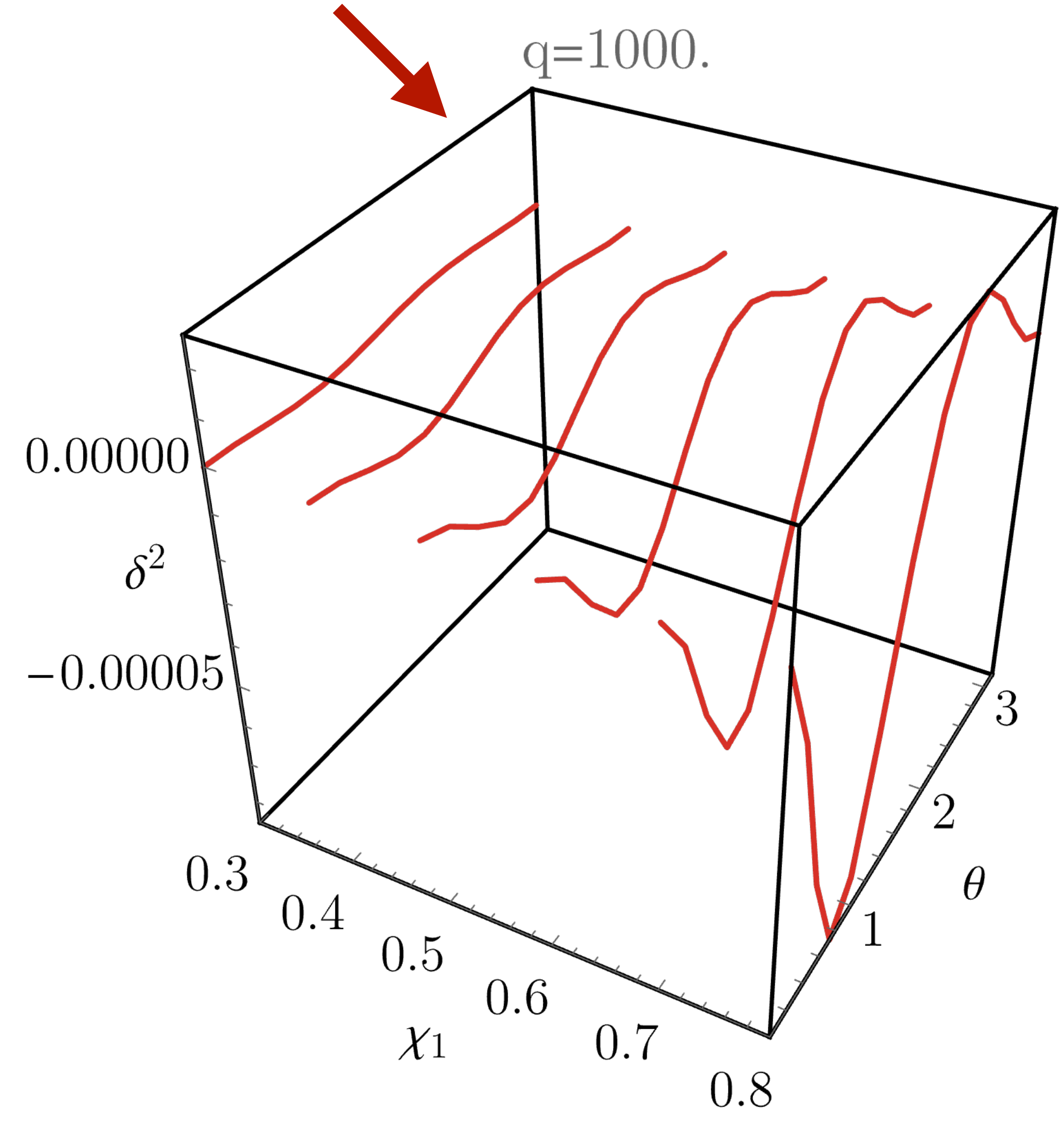

REMNANT PROPERTIES: FINAL SPIN

$$|\chi_f^{\rm prec}| = \sqrt{|\chi_f^{\rm AS}|^2 + \frac{m_1^4}{M_f^4}{\chi_1^{\perp}}^2 + \delta^2}$$

EMRI LIMIT: δ^2 can be obtained **analytically**.

$$|\chi_f^{\rm prec}| = \sqrt{|\chi_f^{\rm AS}|^2 + \frac{m_1^4}{M_f^4}{\chi_1^{\perp}}^2 + \delta^2} \rightarrow$$

$$\boxed{\delta^2 = \frac{m_1^4}{M_f^4}\left[\frac{1}{q^2}(L_z^2 + Q - L_z^{\parallel}) + 2\frac{1}{q}a\cos(I)\left(\sqrt{L_z^2+Q} - L_z^{\parallel}\right)\right]}$$

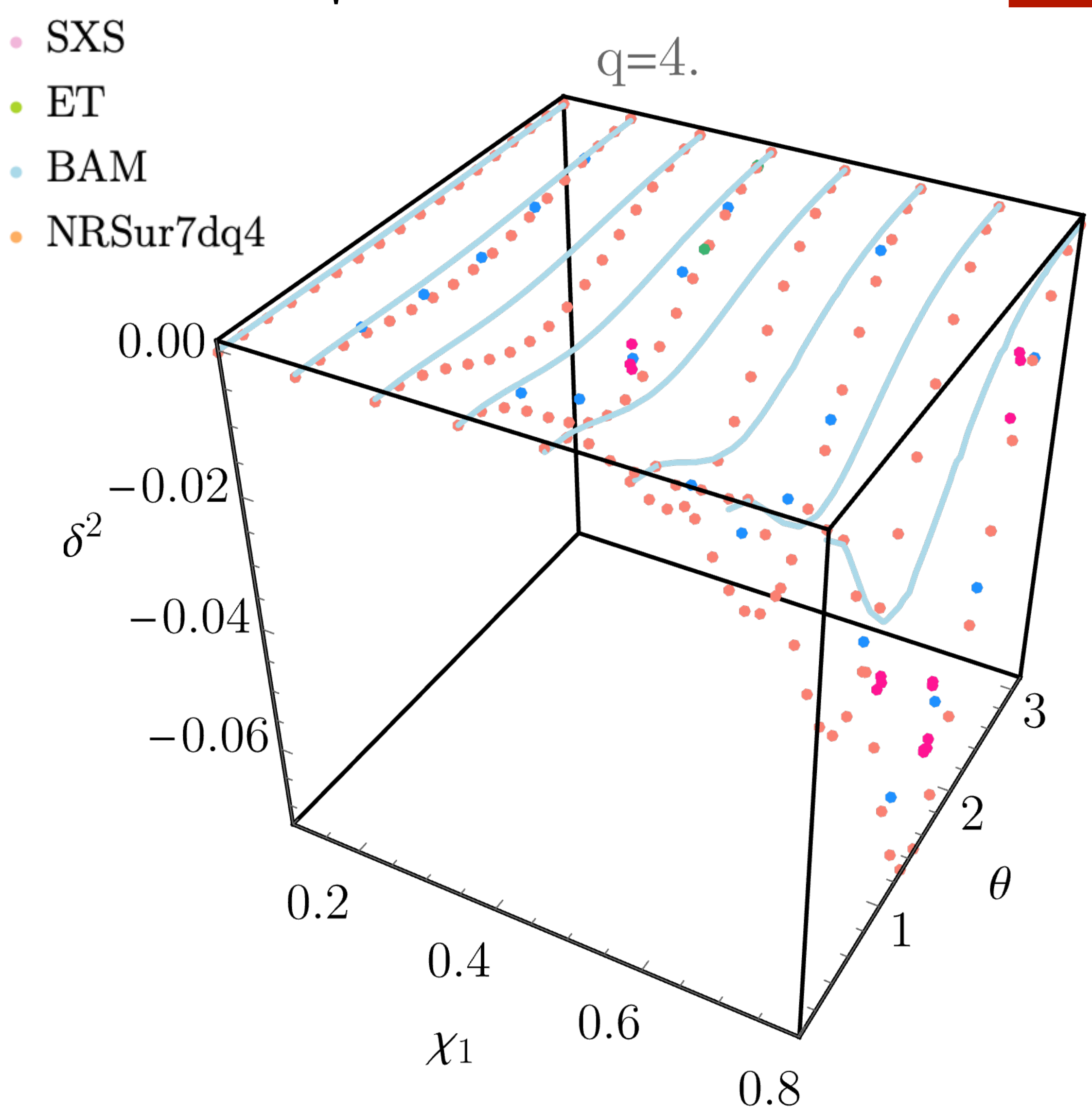

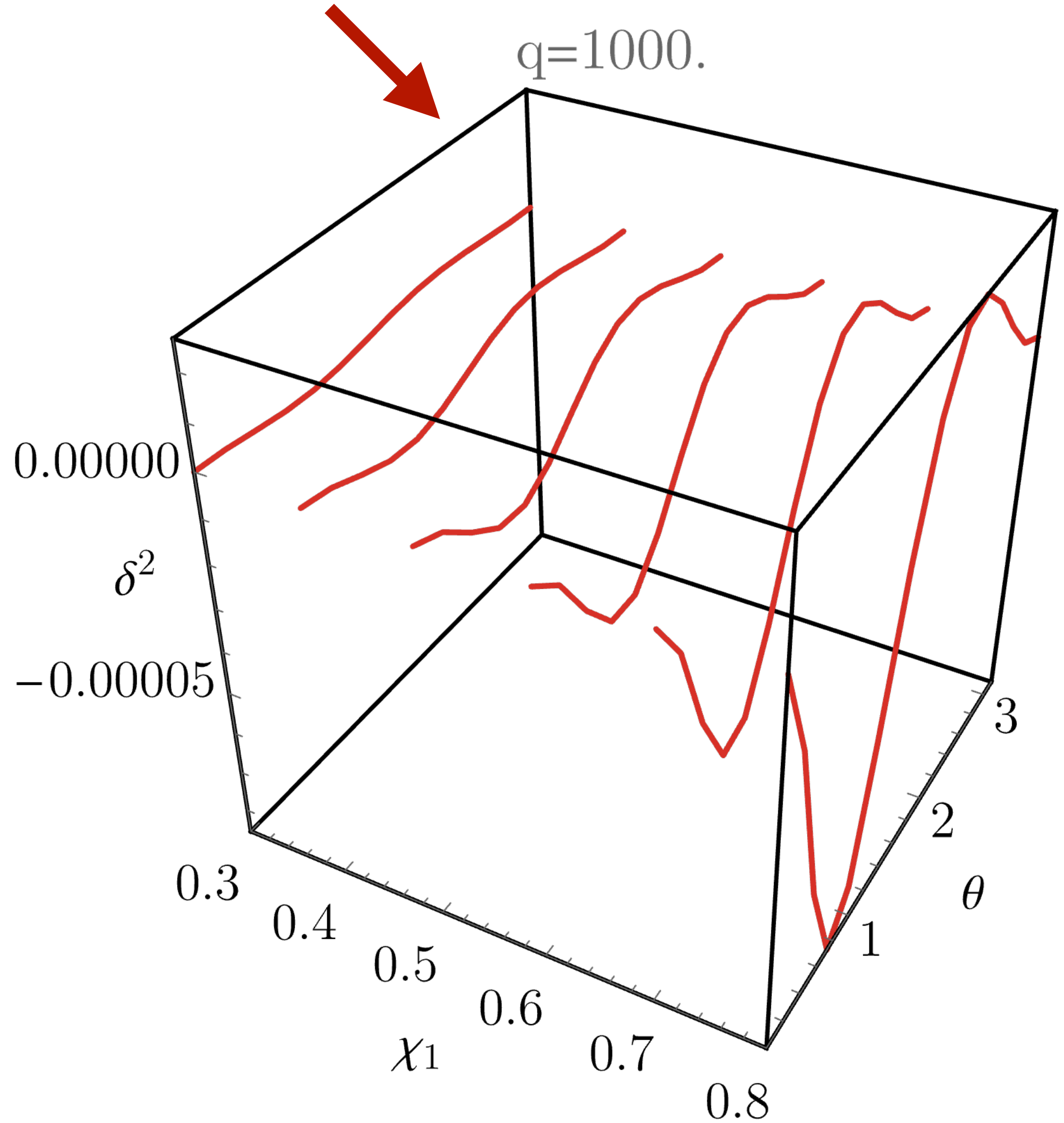

ANALYTICAL EXPRESSION across all η → **shape recovered** even at comparable masses (up to a scale factor).

$$|\chi_f^{\text{prec}}| = \sqrt{|\chi_f^{\text{AS}}|^2 + \frac{m_1^4}{M_f^4}{\chi_1^{\perp}}^2 + \delta^2}$$

Final Spin Magnitude: find fit for δ^2 across the single spin parameter space.

1. **Compute & Plot** δ^2 for fixed θ (θ_f), given by BAM simulations $\left(\frac{\pi}{6}, \frac{\pi}{3}, \frac{\pi}{2}, \frac{2\pi}{3}, \frac{5\pi}{6}\right)$.

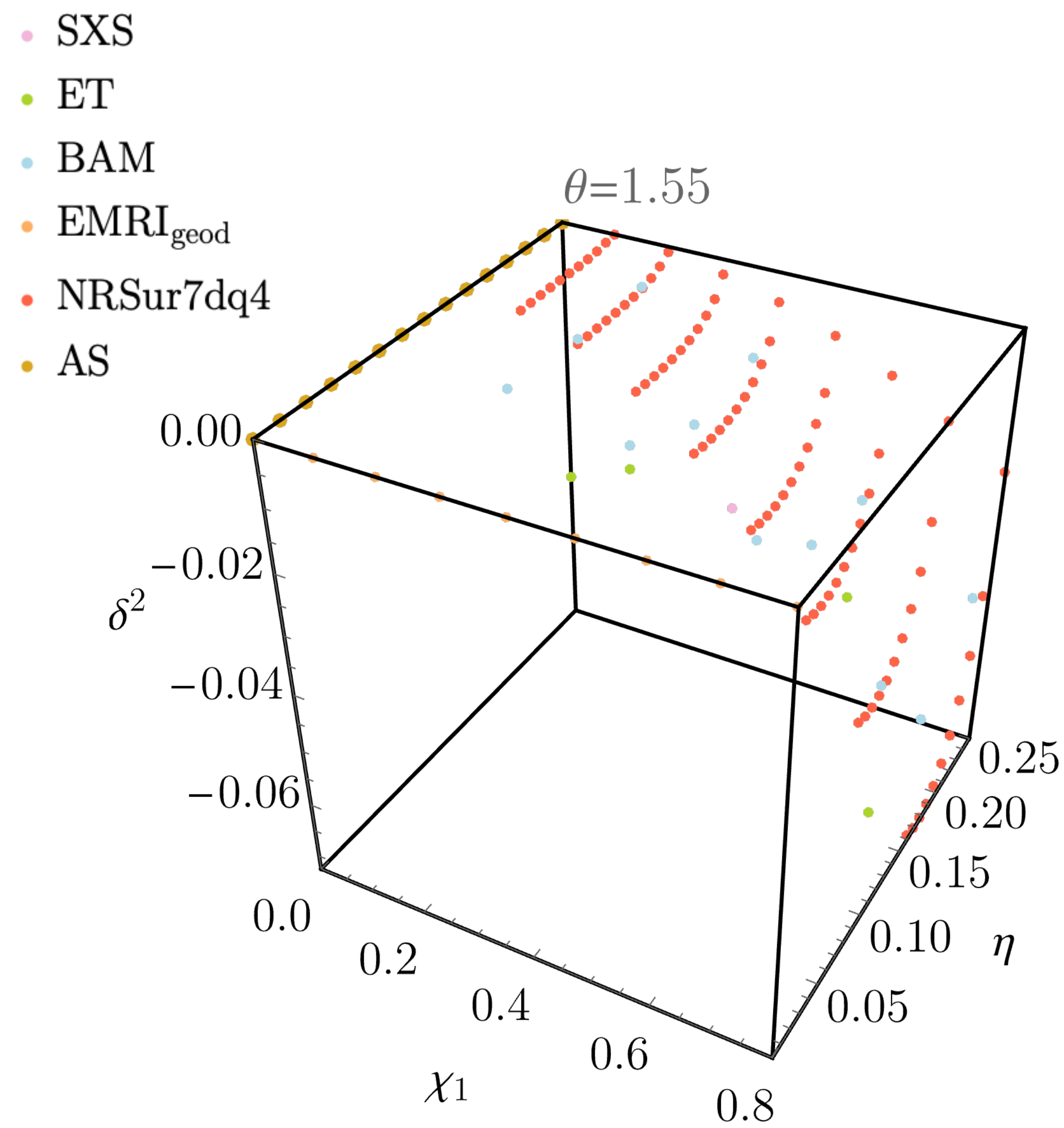

$$|\chi_f^{\text{prec}}| = \sqrt{|\chi_f^{\text{AS}}|^2 + \frac{m_1^4}{M_f^4}\chi_1^{\perp 2} + \delta^2}$$

Final Spin Magnitude: find fit for δ^2 across the single spin parameter space.

1. **Compute & Plot** δ^2 for fixed θ ($\theta_{\rm f}$), given by BAM simulations $\left(\frac{\pi}{6}, \frac{\pi}{3}, \frac{\pi}{2}, \frac{2\pi}{3}, \frac{5\pi}{6}\right)$.

2. **Connect** $q = 4$ to EMRI limit via a 4th order polynomial in η.

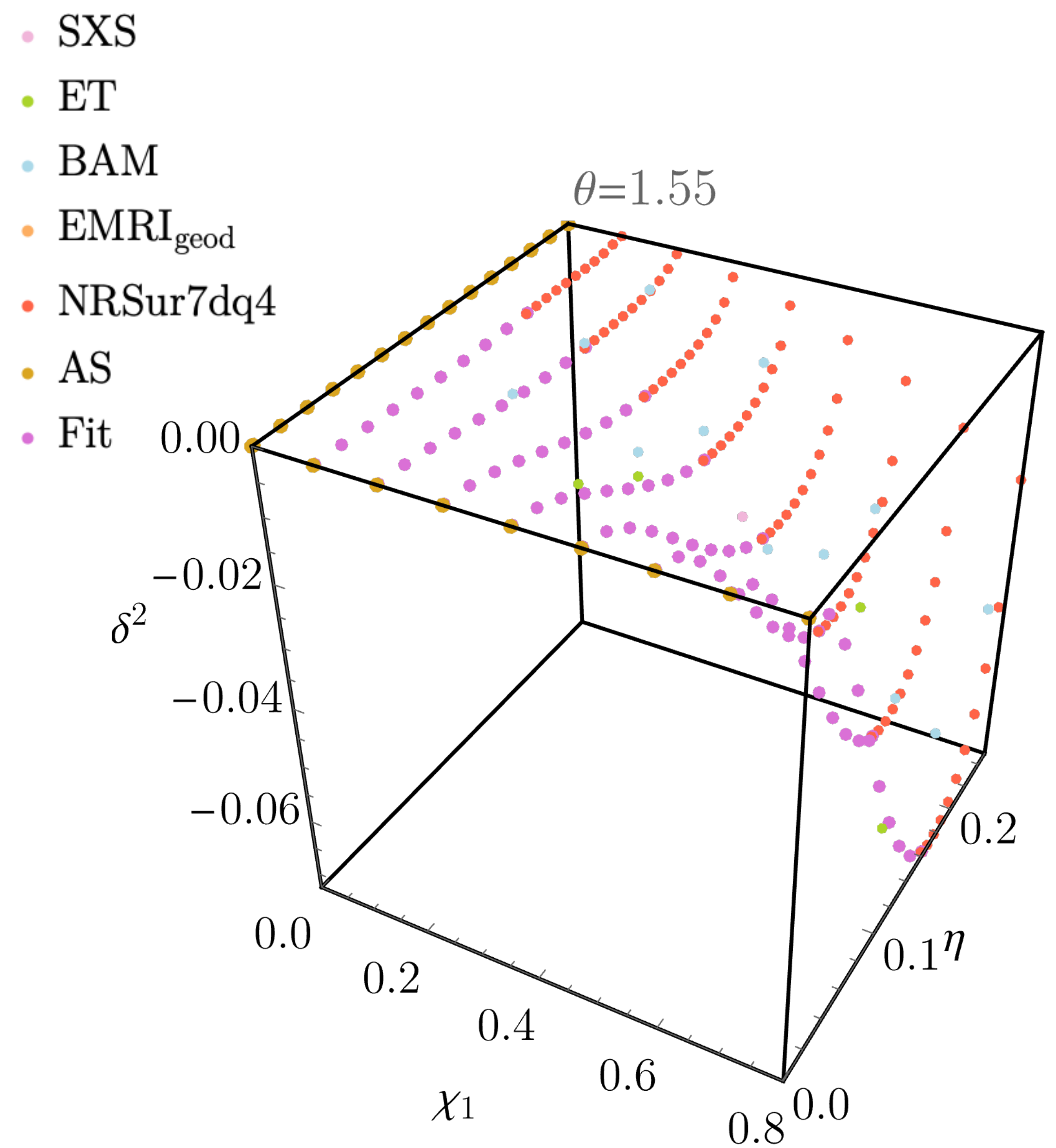

FINAL SPIN MAGNITUDE: find fit for δ^2 across the single spin parameter space.

1. **COMPUTE & PLOT** δ^2 for fixed θ (θ_f), given by BAM simulations $\left(\frac{\pi}{6}, \frac{\pi}{3}, \frac{\pi}{2}, \frac{2\pi}{3}, \frac{5\pi}{6}\right)$.
2. **CONNECT** $q = 4$ to EMRI limit via a 4th order polynomial in η.
3. Perform **FITS** to each $\delta^2(a_i(\theta_f), \eta, \chi_1)$ surface as $\{a_i(\theta_f)\}_{i=1}^{i=9}(\eta^3\chi, \eta^4\chi, \eta^5\chi, \eta^6\chi, \eta^7\chi, \eta^2\chi^2, \eta^3\chi^2, \eta^4\chi^2, \eta^6\chi^2)$.

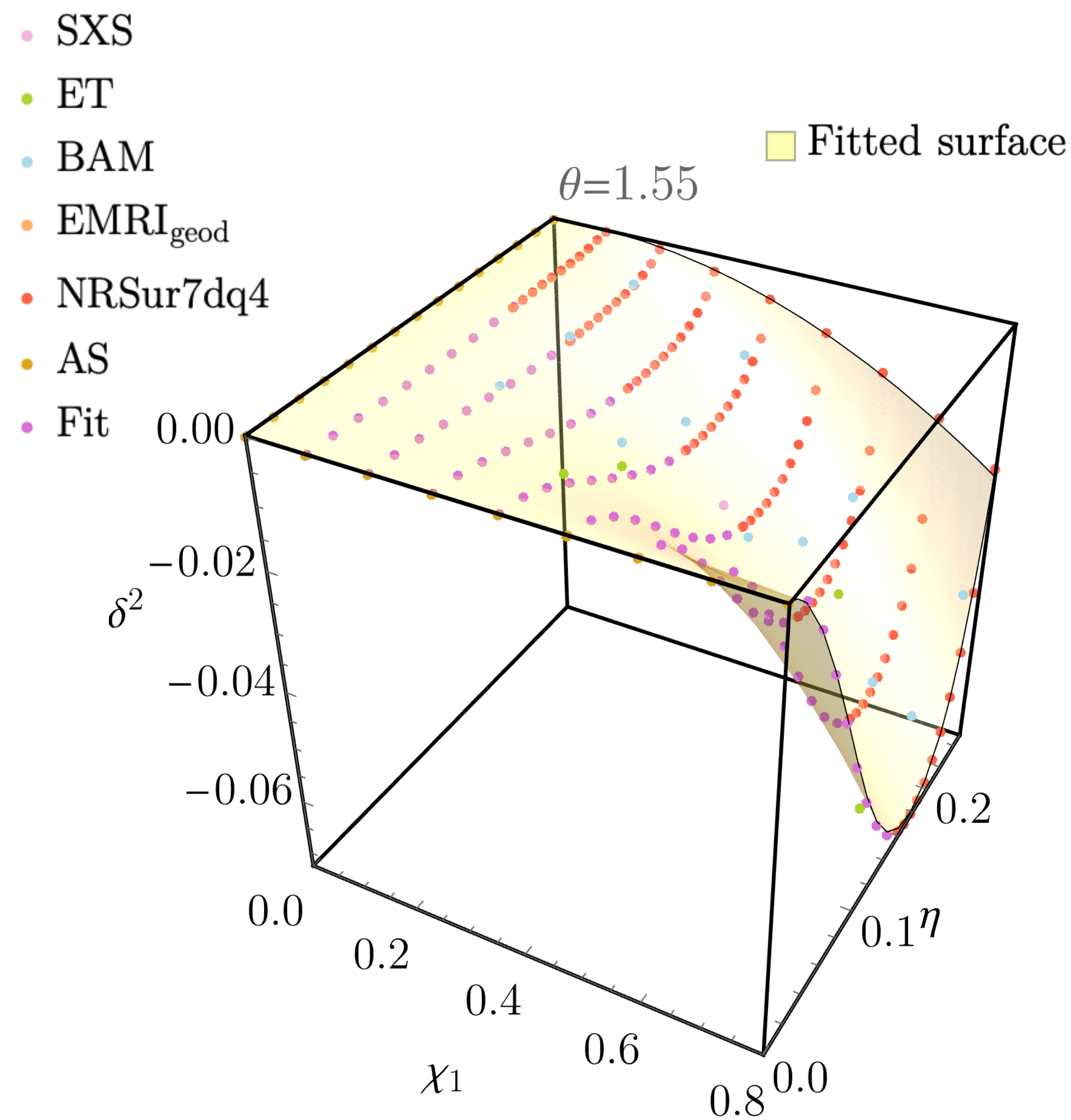

FINAL SPIN MAGNITUDE: find fit for δ^2 across the single spin parameter space.

1. **COMPUTE & PLOT** δ^2 for fixed θ (θ_f), given by BAM simulations $\left(\frac{\pi}{6}, \frac{\pi}{3}, \frac{\pi}{2}, \frac{2\pi}{3}, \frac{5\pi}{6}\right)$.
2. **CONNECT** $q = 4$ to EMRI limit via a 4th order polynomial in η.
3. Perform **FITS** to each $\delta^2(a_i(\theta_\text{f}), \eta, \chi_1)$ surface as $\{a_i(\theta_\text{f})\}_{i=1}^{i=9}\left(\eta^3\chi, \eta^4\chi, \eta^5\chi, \eta^6\chi, \eta^7\chi, \eta^2\chi^2, \eta^3\chi^2, \eta^4\chi^2, \eta^6\chi^2\right)$.
4. Perform **FITS** to each $a_i(\theta)$ via a 5th order polynomial in θ.

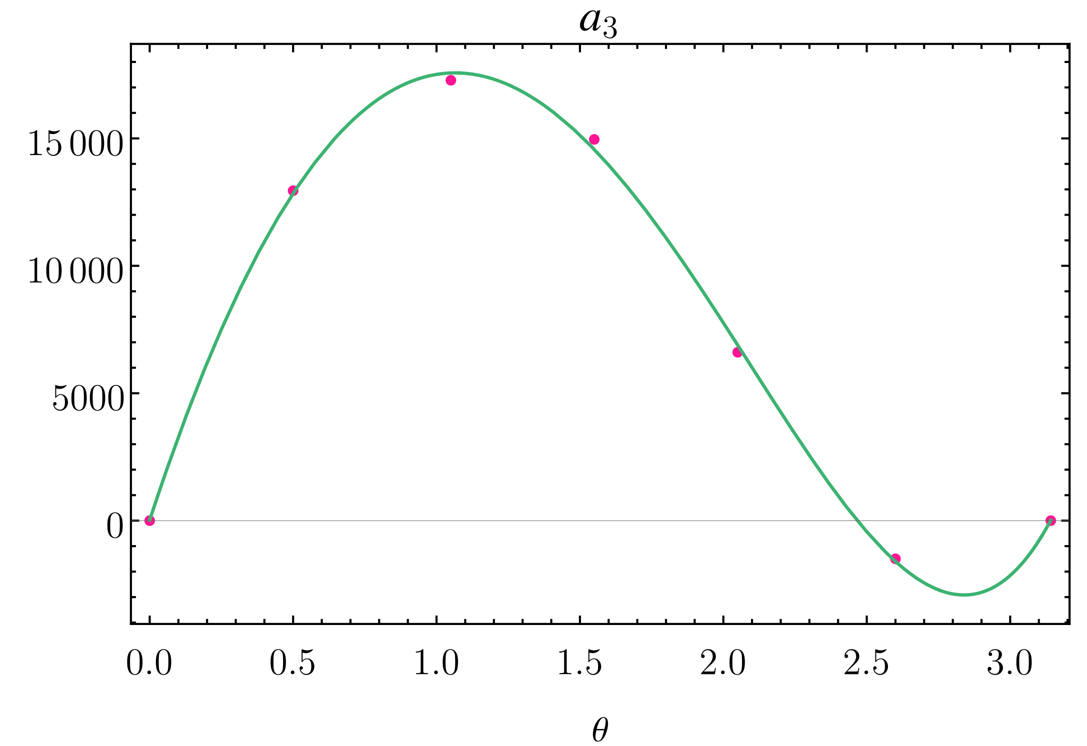

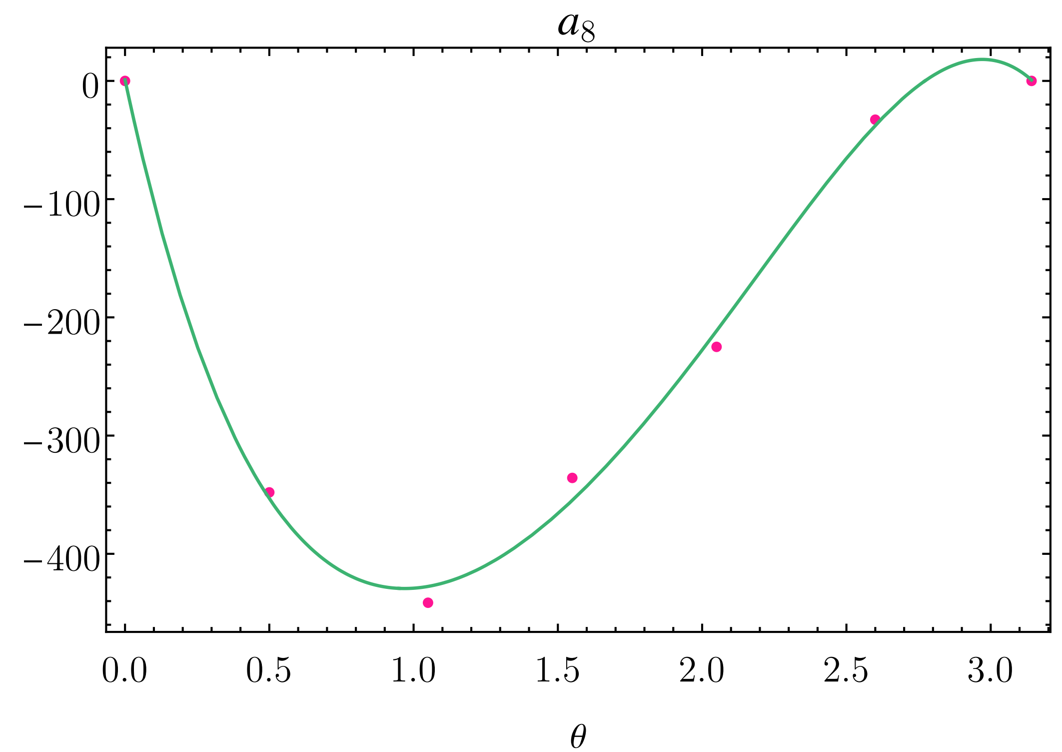

Final Spin Magnitude: find fit for δ^2 across the single spin parameter space.

1. **Compute & Plot** δ^2 for fixed θ ($\theta_{\rm f}$), given by BAM simulations $\left(\frac{\pi}{6}, \frac{\pi}{3}, \frac{\pi}{2}, \frac{2\pi}{3}, \frac{5\pi}{6}\right)$.
2. **Connect** $q = 4$ to EMRI limit via a 4th order polynomial in η.
3. Perform **Fits** to each $\delta^2(a_i(\theta_{\rm f}), \eta, \chi_1)$ surface as $\{a_i(\theta_{\rm f})\}_{i=1}^{i=9}\left(\eta^3\chi, \eta^4\chi, \eta^5\chi, \eta^6\chi, \eta^7\chi, \eta^2\chi^2, \eta^3\chi^2, \eta^4\chi^2, \eta^6\chi^2\right)$.
4. Perform **Fits** to each $a_i(\theta)$ via a 5th order polynomial in θ.
5. Obtain final **Fit** for $\delta^2(a_i(\theta), \eta, \chi_1)$.

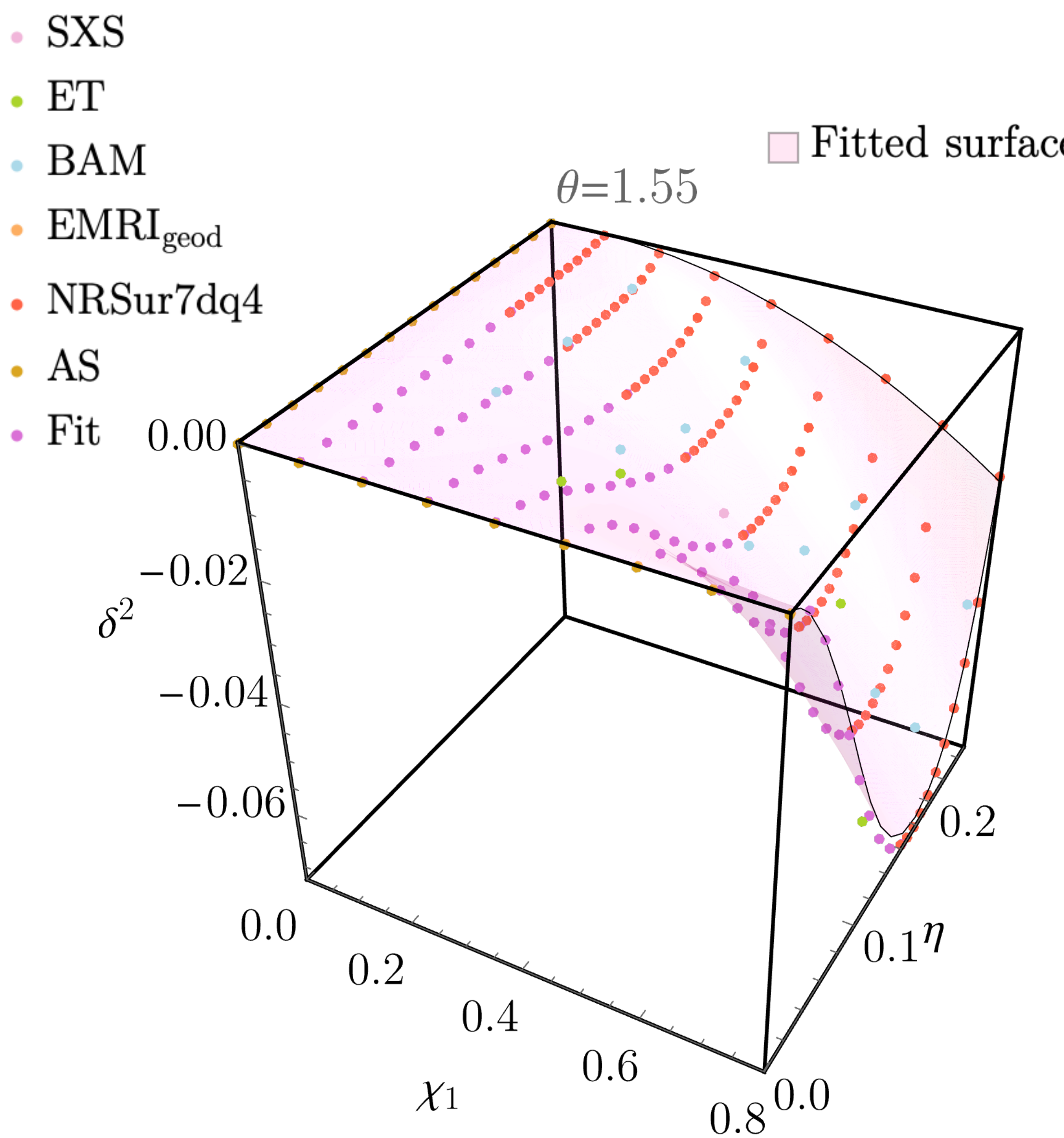

Final Spin Magnitude: find fit for δ^2 across the single spin parameter space.

1. **Compute & Plot** δ^2 for fixed θ (θ_{f}), given by BAM simulations $\left(\frac{\pi}{6}, \frac{\pi}{3}, \frac{\pi}{2}, \frac{2\pi}{3}, \frac{5\pi}{6}\right)$.
2. **Connect** $q = 4$ to EMRI limit via a 4th order polynomial in η.
3. Perform **Fits** to each $\delta^2(a_i(\theta_{\text{f}}), \eta, \chi_1)$ surface as $\{a_i(\theta_{\text{f}})\}_{i=1}^{i=9}(\eta^3\chi, \eta^4\chi, \eta^5\chi, \eta^6\chi, \eta^7\chi, \eta^2\chi^2, \eta^3\chi^2, \eta^4\chi^2, \eta^6\chi^2)$.
4. Perform **Fits** to each $a_i(\theta)$ via a 5th order polynomial in θ.
5. Obtain final **Fit** for $\delta^2(a_i(\theta), \eta, \chi_1)$.
6. Check the **Accuracy** of the new model compared to `NRSur7dq4` and `PhenXP`.

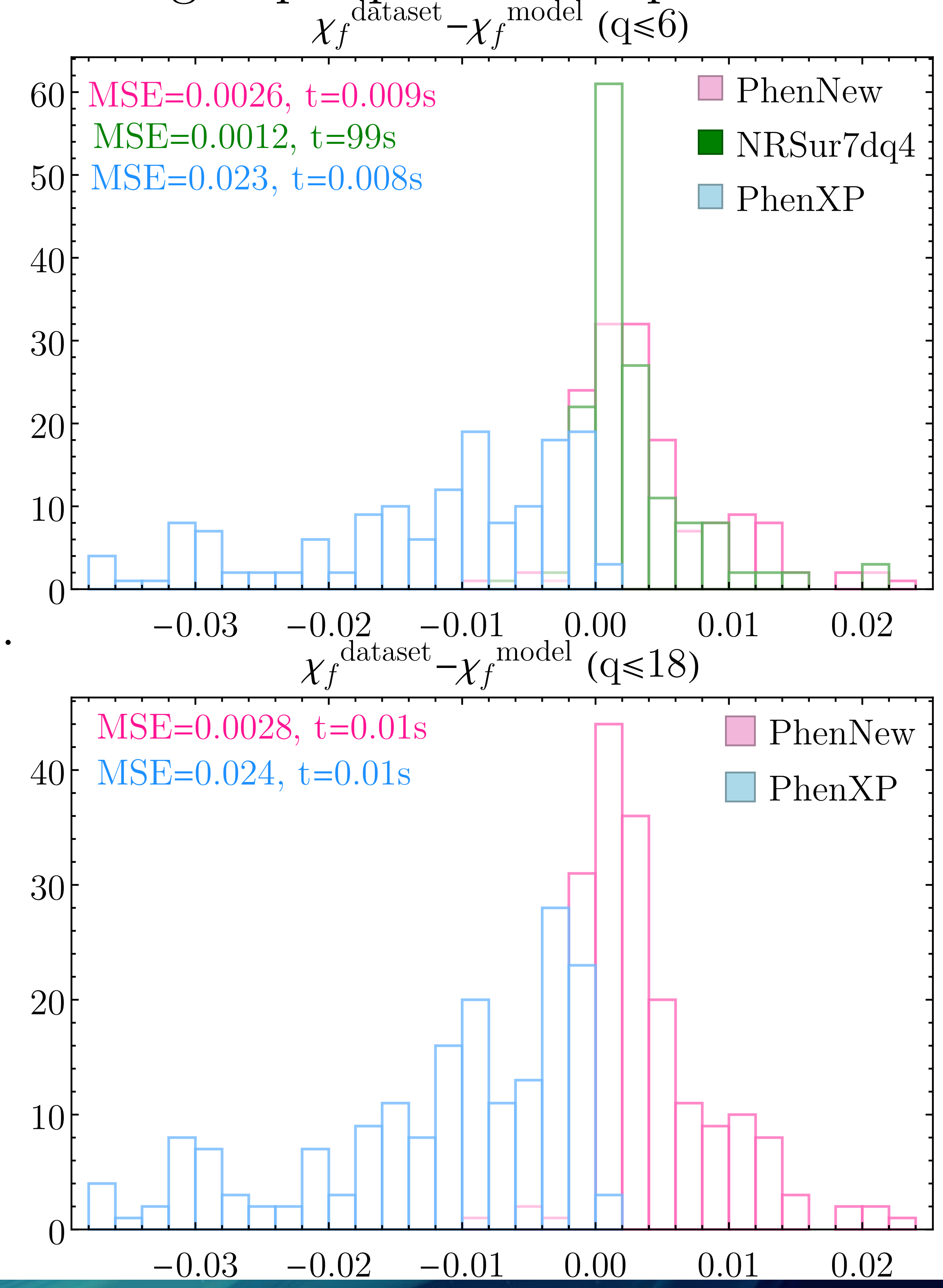

Radiated Energy: find fit for ΔE across the single spin parameter space.

1. **Improve** current $E_{\rm rad}^{AS}$ fit from `PhenX` to **capture the EMRI** limit.

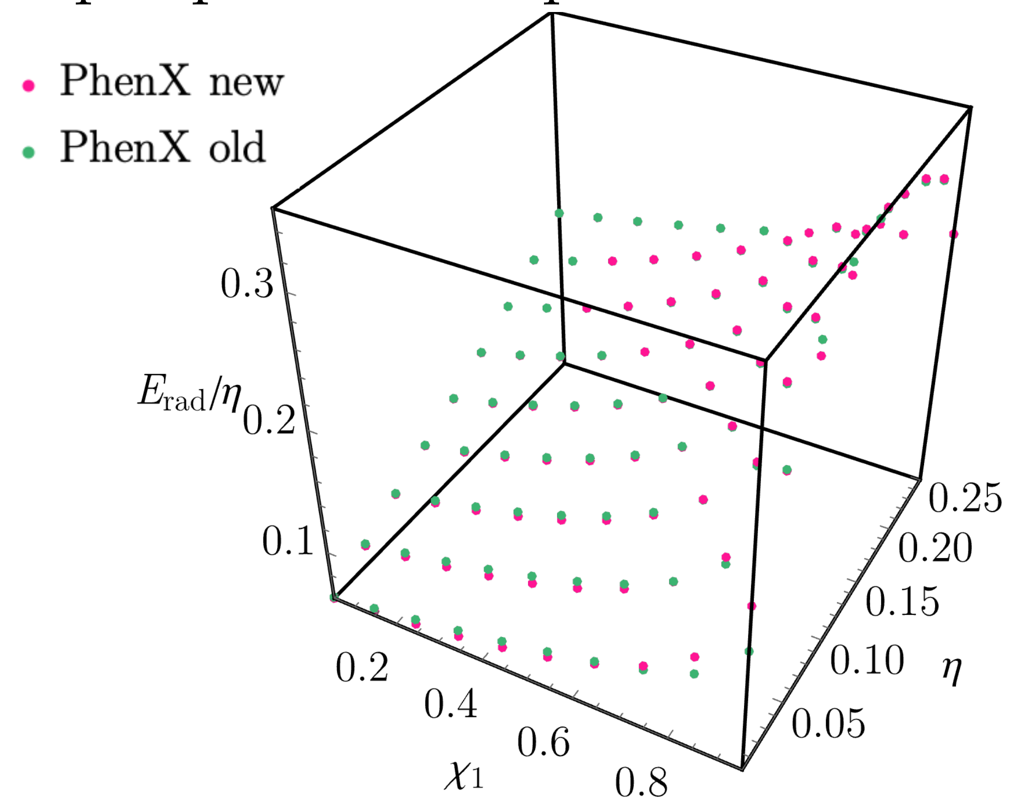

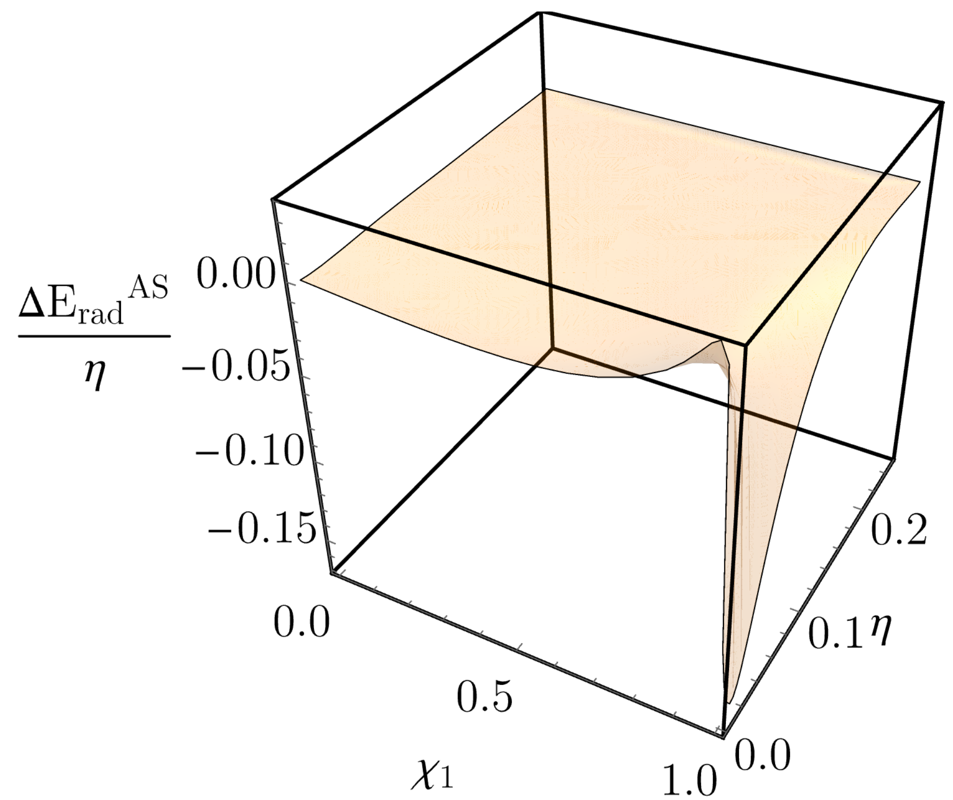

RADIATED ENERGY: find fit for ΔE across the single spin parameter space.

1. **IMPROVE** current $E^{AS}_{\rm rad}$ fit from `PhenX` to **capture the EMRI** limit.
2. **COMPUTE & PLOT** ΔE for fixed θ ($\theta_{\rm f}$), given by BAM simulations $\left(\frac{\pi}{6}, \frac{\pi}{3}, \frac{\pi}{2}, \frac{2\pi}{3}, \frac{5\pi}{6}\right)$.

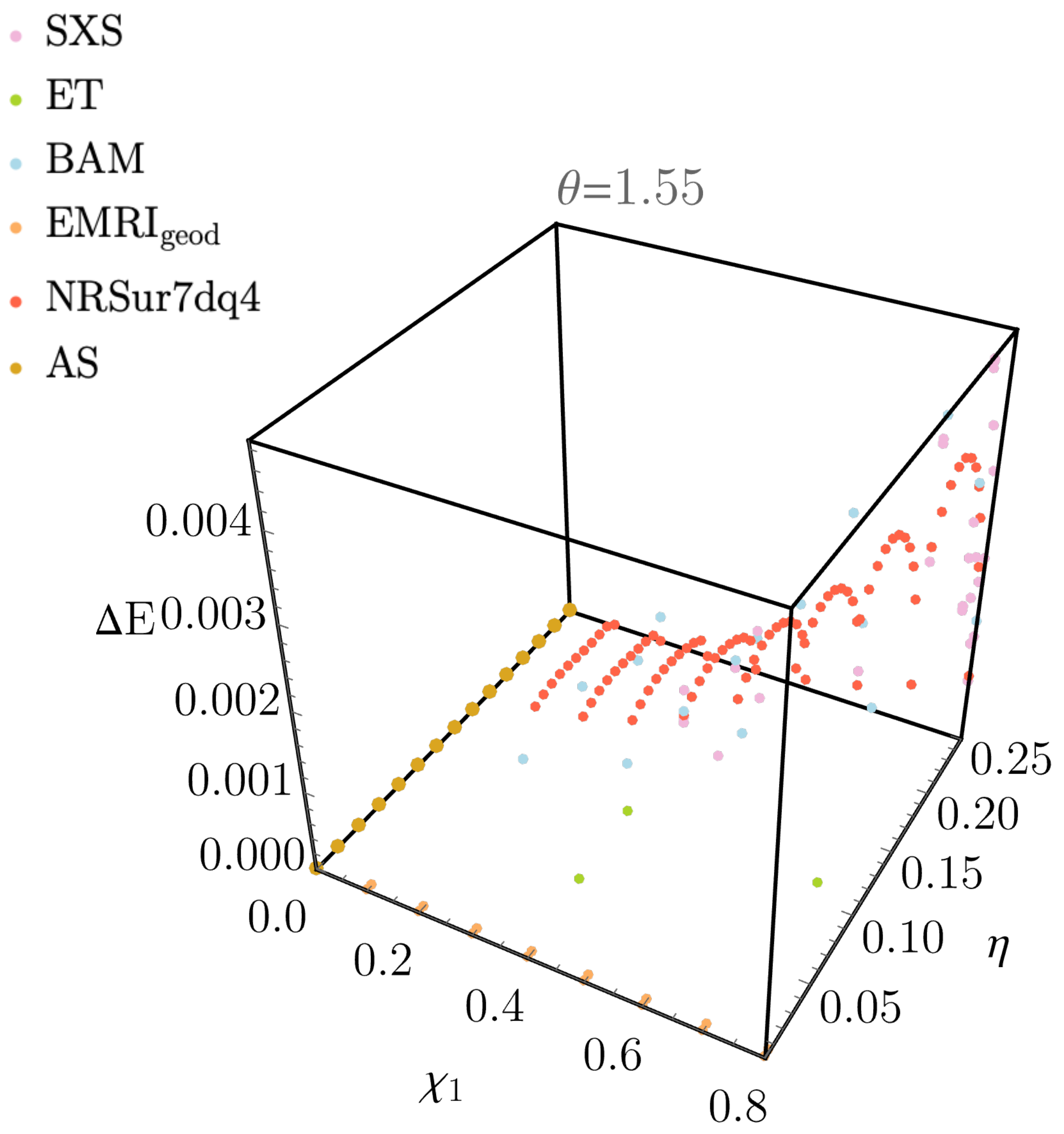

Radiated Energy: find fit for ΔE across the single spin parameter space.

1. **Improve** current E_{rad}^{AS} fit from `PhenX` to **capture the EMRI** limit.
2. **Compute & Plot** ΔE for fixed θ (θ_{f}), given by BAM simulations $\left(\frac{\pi}{6}, \frac{\pi}{3}, \frac{\pi}{2}, \frac{2\pi}{3}, \frac{5\pi}{6}\right)$.
3. **Connect** $q = 4$ to EMRI limit via a 4th order polynomial in η.

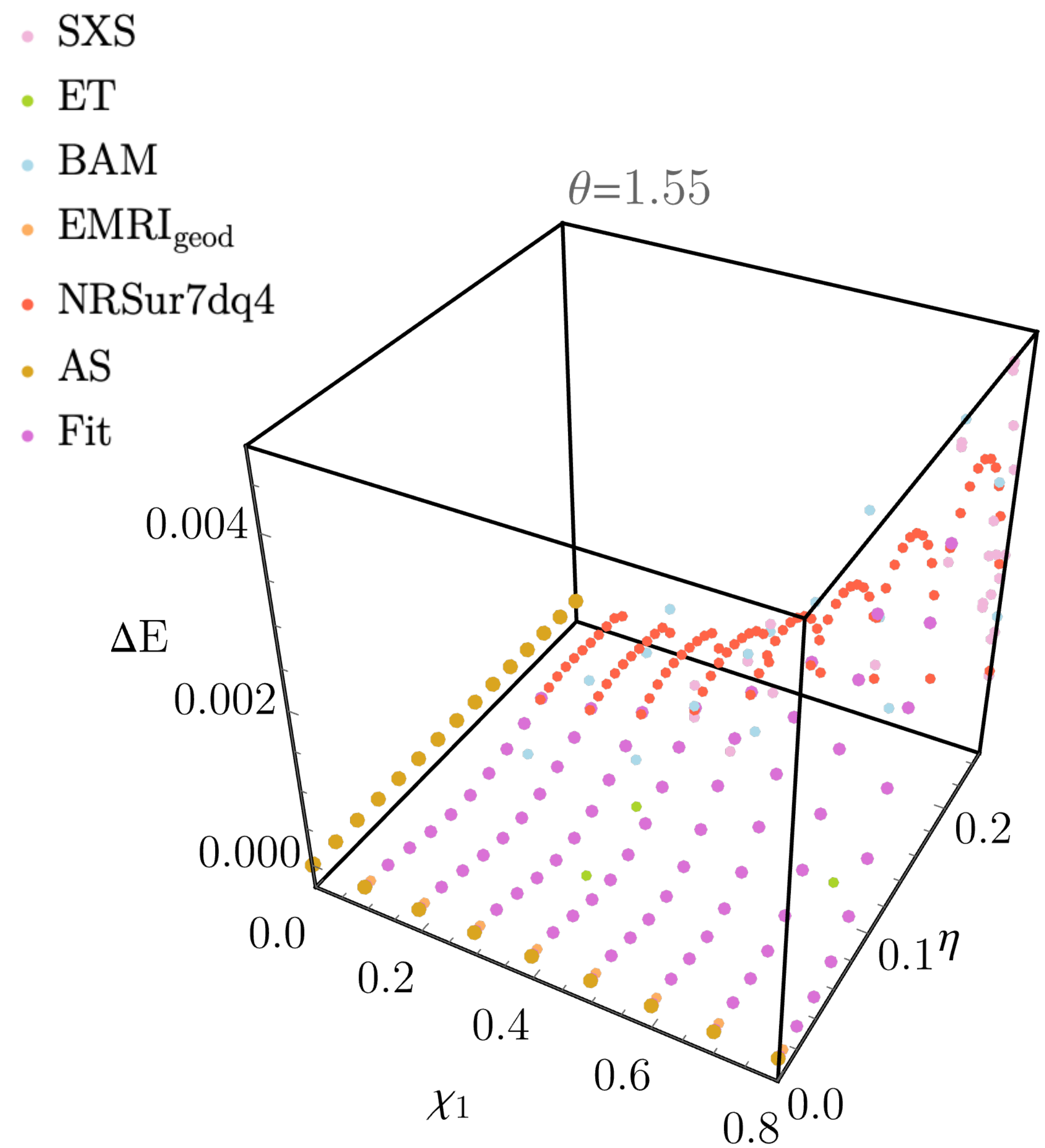

 $\Delta E = E^{\rm prec}_{\rm rad}\left(q, |\chi_1|, \theta_{\vec{\chi}_1,\vec{L}}\right) - E^{\rm AS}_{\rm rad}\left(q, |\chi_1|\cos(\theta_{\vec{\chi}_1,\vec{L}})\right)$

Radiated Energy: find fit for ΔE across the single spin parameter space.

1. **Improve** current $E^{AS}_{\rm rad}$ fit from `PhenX` to **capture the EMRI** limit.
2. **Compute & Plot** ΔE for fixed θ ($\theta_{\rm f}$), given by BAM simulations $\left(\frac{\pi}{6}, \frac{\pi}{3}, \frac{\pi}{2}, \frac{2\pi}{3}, \frac{5\pi}{6}\right)$.
3. **Connect** $q = 4$ to EMRI limit via a 4th order polynomial in η.
4. Perform **Fits** to each $\Delta E(a_i(\theta_{\rm f}), \eta, \chi_1)$ surface as $\{a_i(\theta_{\rm f})\}_{i=1}^{i=9}(\eta^3\chi, \eta^4\chi, \eta^5\chi, \eta^6\chi, \eta^7\chi, \eta^2\chi^2, \eta^3\chi^2, \eta^4\chi^2, \eta^6\chi^2)$.

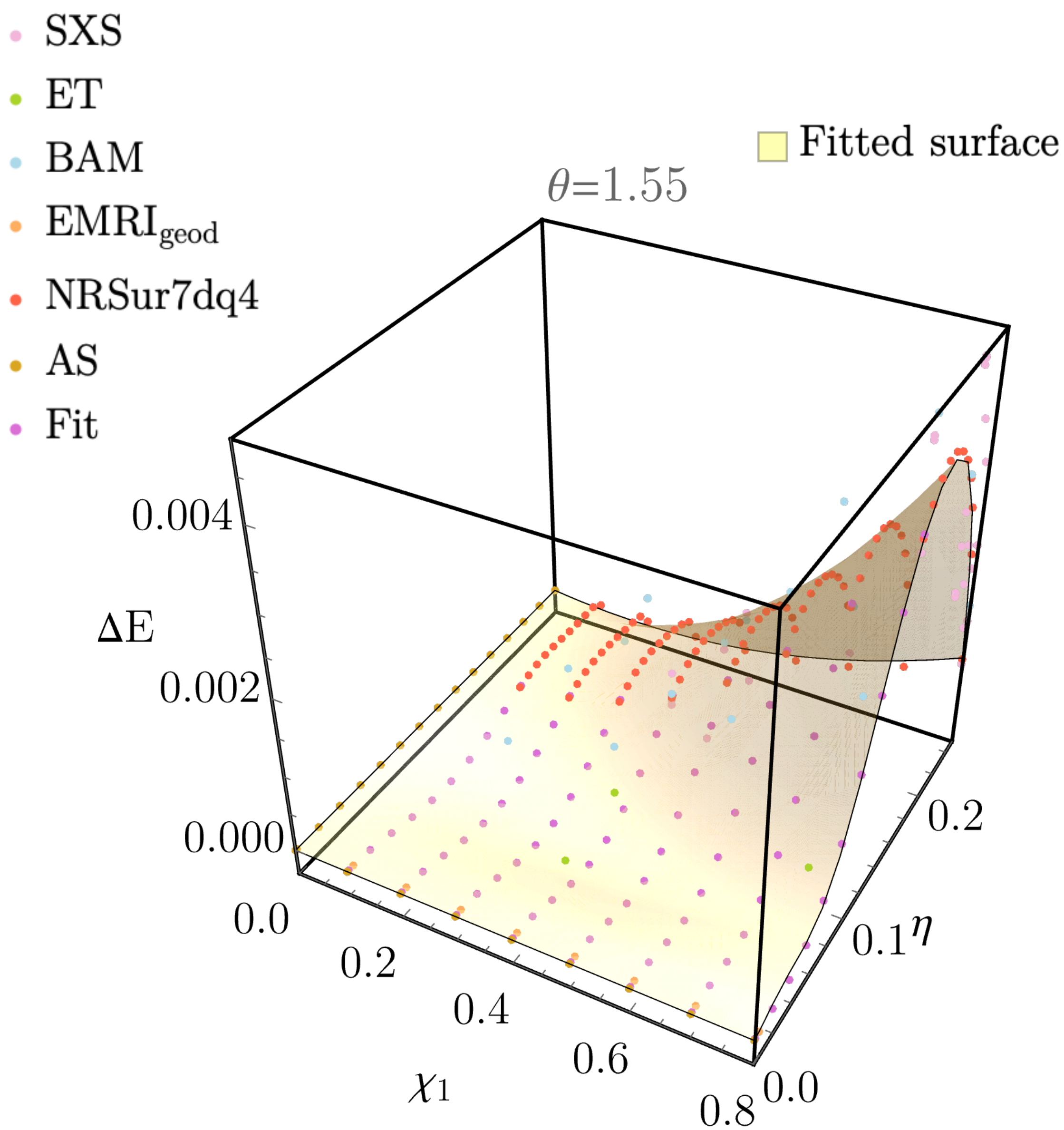

Radiated Energy: find fit for ΔE across the single spin parameter space.

1. **Improve** current E_{rad}^{AS} fit from `PhenX` to **capture the EMRI** limit.
2. **Compute & Plot** ΔE for fixed θ (θ_{f}), given by BAM simulations $\left(\frac{\pi}{6}, \frac{\pi}{3}, \frac{\pi}{2}, \frac{2\pi}{3}, \frac{5\pi}{6}\right)$.
3. **Connect** $q = 4$ to EMRI limit via a 4th order polynomial in η.
4. Perform **Fits** to each $\Delta E(a_i(\theta_{\text{f}}), \eta, \chi_1)$ surface as $\{a_i(\theta_{\text{f}})\}_{i=1}^{i=9}\left(\eta^3\chi, \eta^4\chi, \eta^5\chi, \eta^6\chi, \eta^7\chi, \eta^2\chi^2, \eta^3\chi^2, \eta^4\chi^2, \eta^6\chi^2\right)$.
5. Perform **Fits** to each $a_i(\theta)$ via a 5th order polynomial in θ.

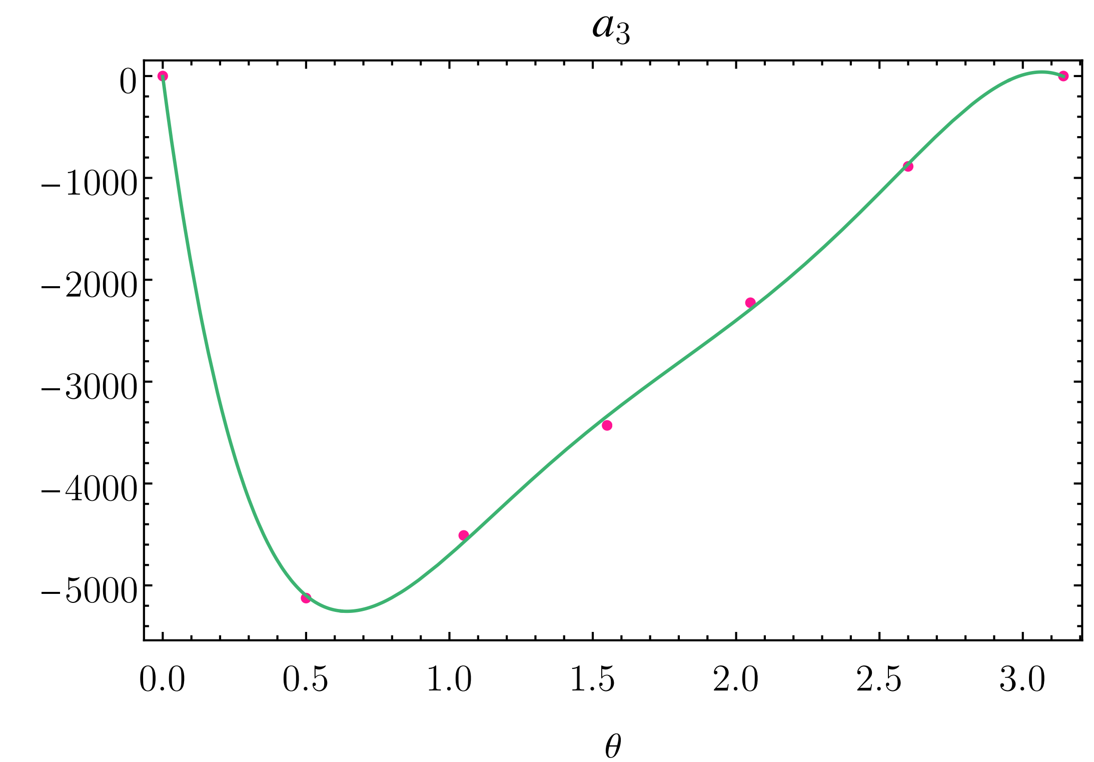

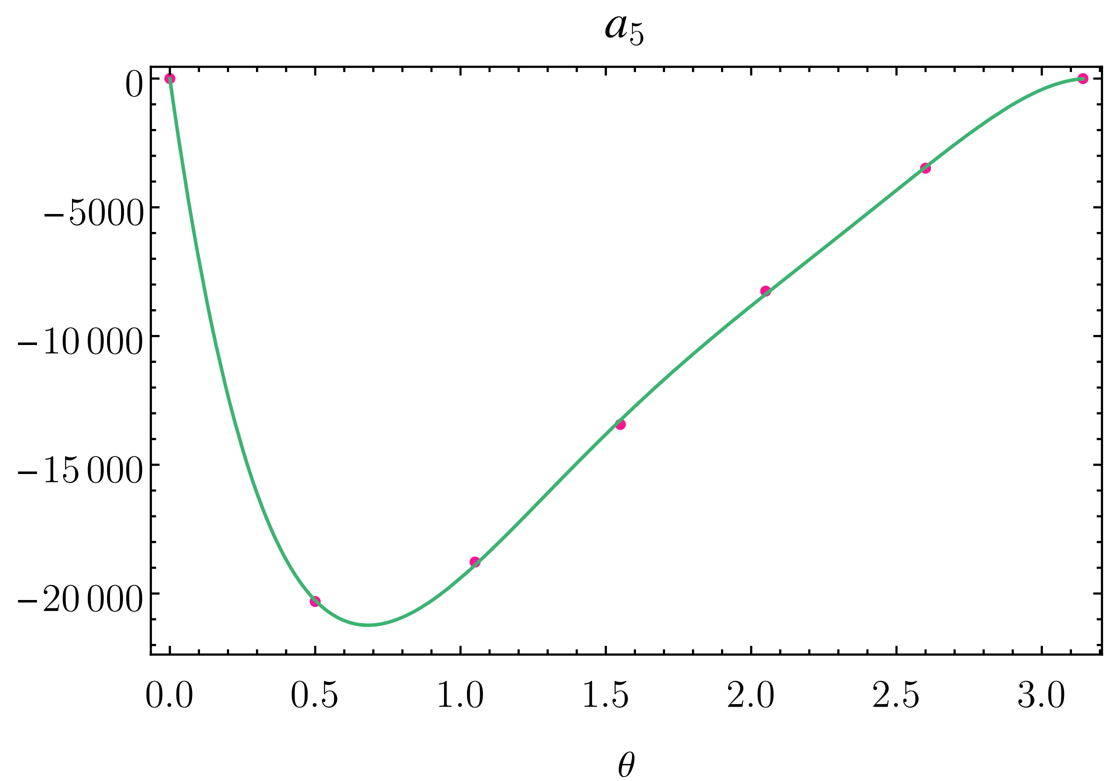

RADIATED ENERGY: find fit for ΔE across the single spin parameter space.

1. **IMPROVE** current $E^{AS}_{\rm rad}$ fit from `PhenX` to **capture the EMRI** limit.
2. **COMPUTE & PLOT** ΔE for fixed θ ($\theta_{\rm f}$), given by BAM simulations $\left(\frac{\pi}{6}, \frac{\pi}{3}, \frac{\pi}{2}, \frac{2\pi}{3}, \frac{5\pi}{6}\right)$.
3. **CONNECT** $q = 4$ to EMRI limit via a 4th order polynomial in η.
4. Perform **FITS** to each $\Delta E(a_i(\theta_{\rm f}), \eta, \chi_1)$ surface as $\{a_i(\theta_{\rm f})\}_{i=1}^{i=9}\left(\eta^3\chi, \eta^4\chi, \eta^5\chi, \eta^6\chi, \eta^7\chi, \eta^2\chi^2, \eta^3\chi^2, \eta^4\chi^2, \eta^6\chi^2\right)$.
5. Perform **FITS** to each $a_i(\theta)$ via a 5th order polynomial in θ.
6. Obtain final **FIT** for $\Delta E(a_i(\theta), \eta, \chi_1)$.

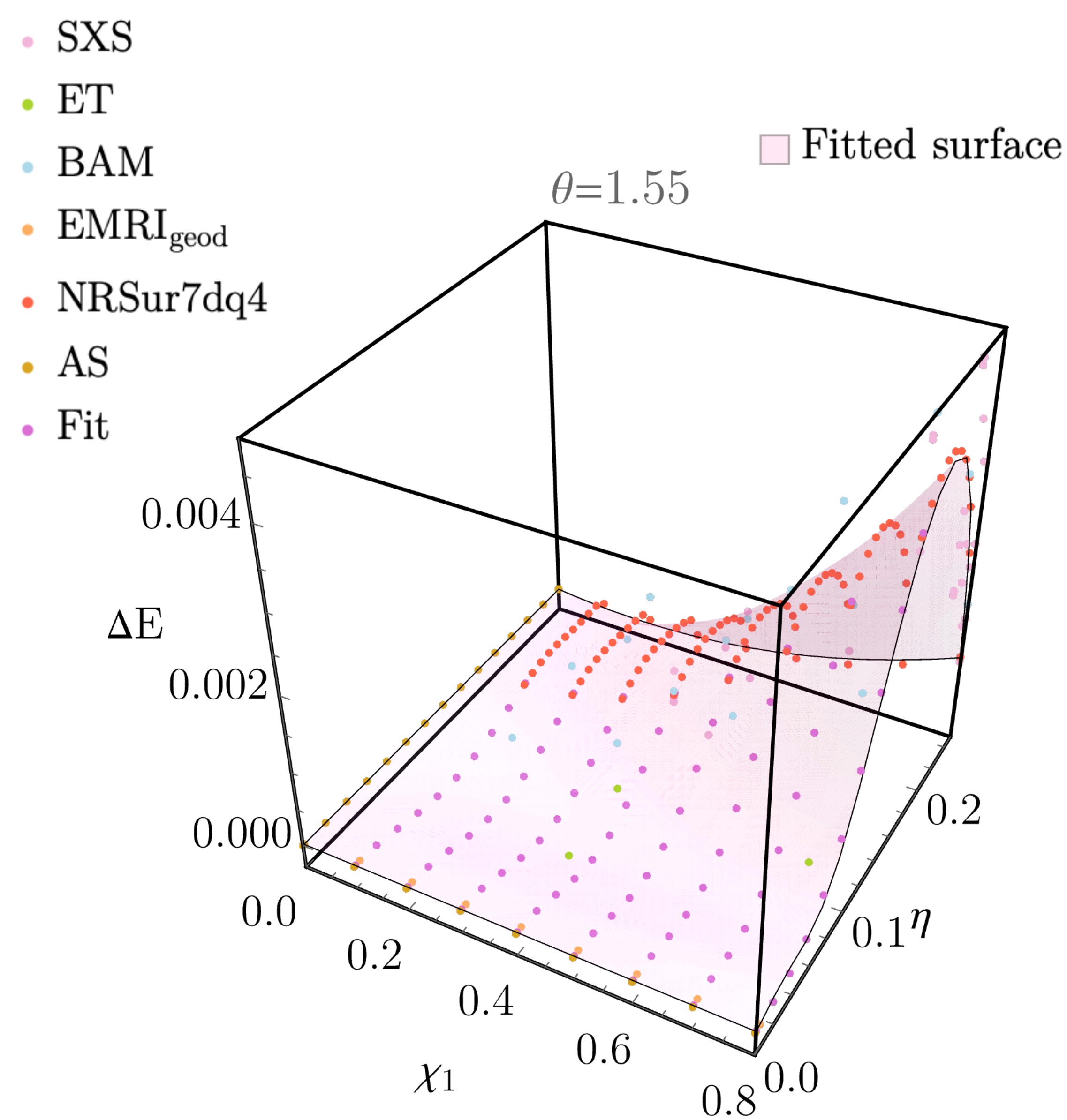

RADIATED ENERGY: find fit for ΔE across the single spin parameter space.

1. **IMPROVE** current $E^{AS}_{\rm rad}$ fit from `PhenX` to **capture the EMRI** limit.
2. **COMPUTE & PLOT** ΔE for fixed θ ($\theta_{\rm f}$), given by BAM simulations $\left(\frac{\pi}{6}, \frac{\pi}{3}, \frac{\pi}{2}, \frac{2\pi}{3}, \frac{5\pi}{6}\right)$.
3. **CONNECT** $q = 4$ to EMRI limit via a 4th order polynomial in η.
4. Perform **FITS** to each $\Delta E(a_i(\theta_{\rm f}), \eta, \chi_1)$ surface as $\{a_i(\theta_{\rm f})\}_{i=1}^{i=9}(\eta^3\chi, \eta^4\chi, \eta^5\chi, \eta^6\chi, \eta^7\chi, \eta^2\chi^2, \eta^3\chi^2, \eta^4\chi^2, \eta^6\chi^2)$.
5. Perform **FITS** to each $a_i(\theta)$ via a 5th order polynomial in θ.
6. Obtain final **FIT** for $\Delta E(a_i(\theta), \eta, \chi_1)$.
7. Check the **ACCURACY** of the new model compared to `NRSur7dq4` and `PhenXP`.

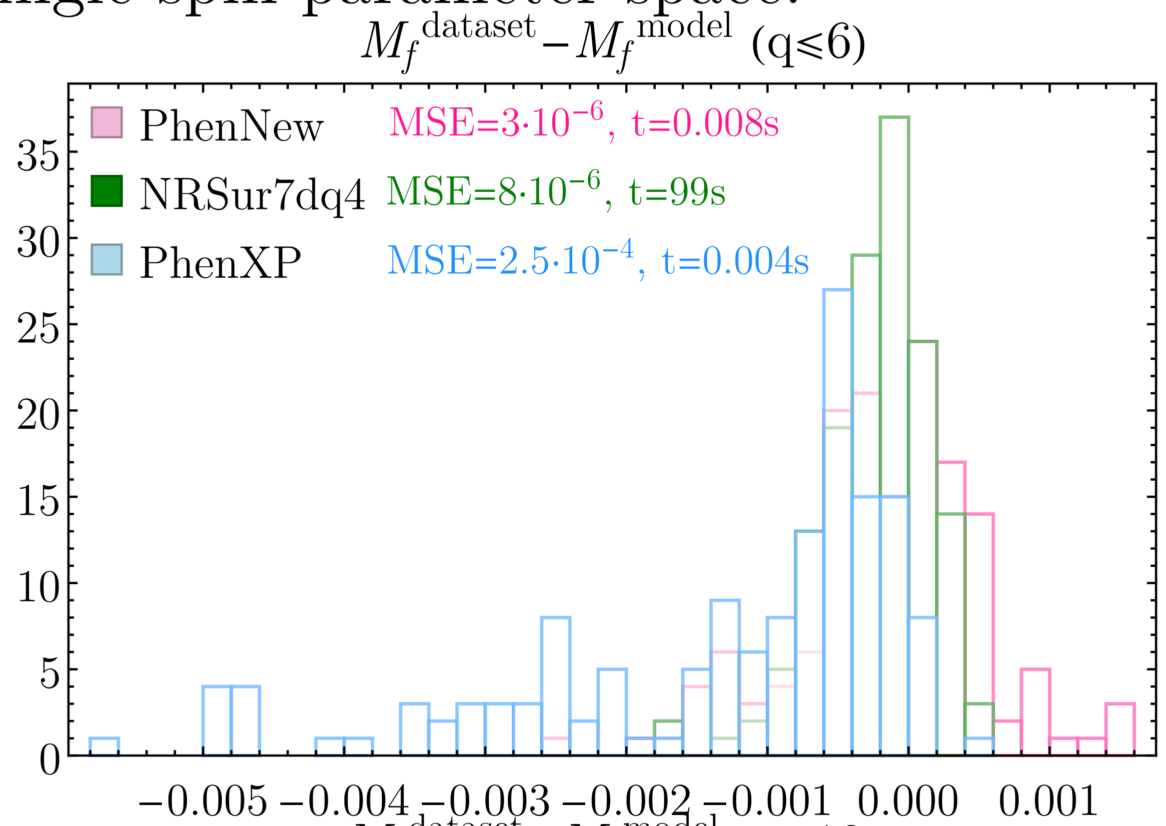

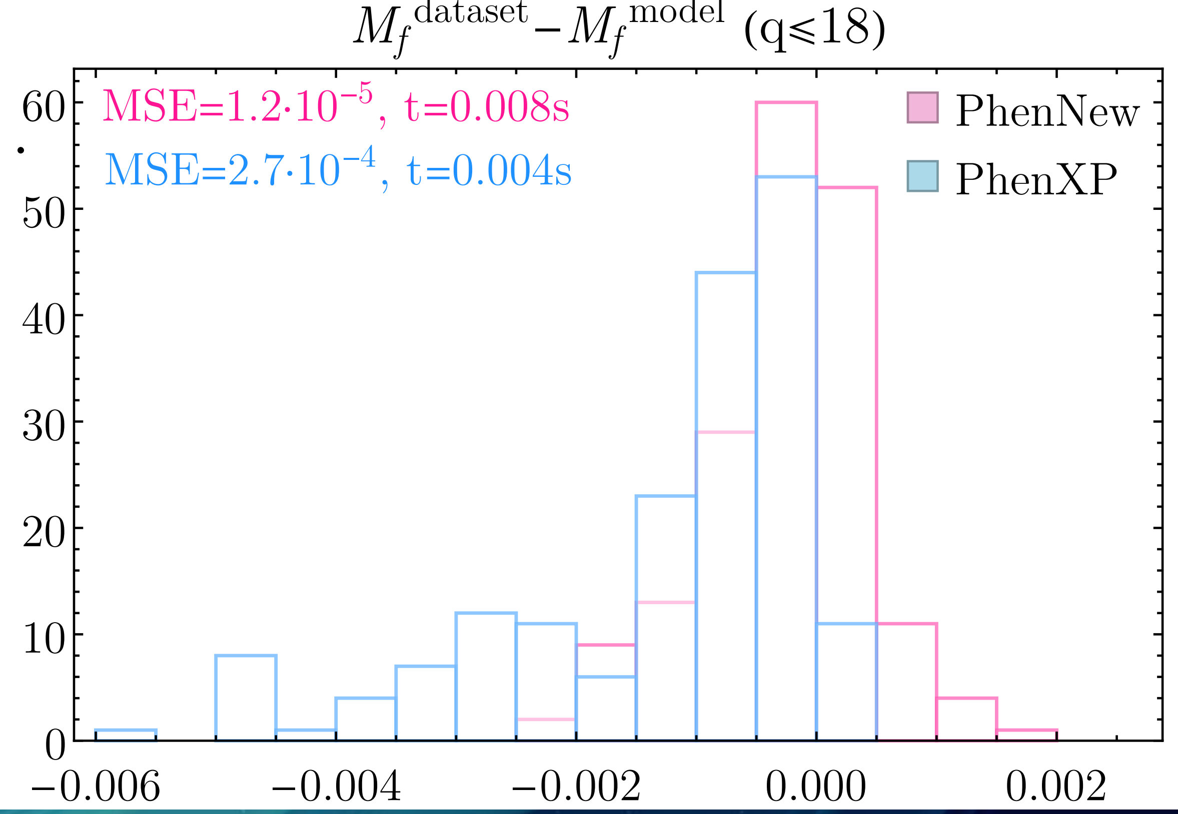

Conclusions

- **High dimensionality** of Precessing Systems → NR informed models are challenging.

Conclusions

- **High dimensionality** of Precessing Systems → NR informed models are challenging.
    - Not enough NR Simulations to densely **cover** the 7-dim parameter space.

Conclusions

- **High dimensionality** of Precessing Systems → NR informed models are challenging.
    - Not enough NR Simulations to densely **cover** the 7-dim parameter space.
    - High q Simulations are computationally **expensive**: no NR information for $q > 18$.

Conclusions

- **High dimensionality** of Precessing Systems → NR informed models are challenging.
  - Not enough NR Simulations to densely **cover** the 7-dim parameter space.
  - High q Simulations are computationally **expensive**: no NR information for $q > 18$.
  - The Emri Limit has to be used to **reduce the number** of NR simulations needed.

Conclusions

- **High dimensionality** of Precessing Systems → NR informed models are challenging.
  - Not enough NR Simulations to densely **cover** the 7-dim parameter space.
  - High q Simulations are computationally **expensive**: no NR information for $q > 18$.
  - The Emri Limit has to be used to **reduce the number** of NR simulations needed.
- We Created a **consistent and heterogeneous dataset** for quasi-circular precessing binaries, combining NR waveforms, NRSur7dq4 and the EMRI limit.

CONCLUSIONS

- **High dimensionality** of PRECESSING SYSTEMS → NR informed models are challenging.
  - NOT ENOUGH NR SIMULATIONS to densely **cover** the 7-dim parameter space.
  - HIGH q SIMULATIONS are computationally **expensive**: no NR information for $q > 18$.
  - The EMRI LIMIT has to be used to **reduce the number** of NR simulations needed.
- We CREATED a **consistent and heterogeneous dataset** for quasi-circular precessing binaries, combining NR waveforms, NRSur7dq4 and the EMRI limit.
- We GENERATED fits for the **remnant properties** for the single spin across the η-dimension more accurate than `PhenXP` and faster than `NRSur7dq4`.

Conclusions

- **High dimensionality** of Precessing Systems → NR informed models are challenging.
    - Not enough NR Simulations to densely **cover** the 7-dim parameter space.
    - High q Simulations are computationally **expensive**: no NR information for $q > 18$.
    - The Emri Limit has to be used to **reduce the number** of NR simulations needed.
- We Created a **consistent and heterogeneous dataset** for quasi-circular precessing binaries, combining NR waveforms, NRSur7dq4 and the EMRI limit.
- We Generated fits for the **remnant properties** for the single spin across the η-dimension more accurate than `PhenXP` and faster than `NRSur7dq4`.
    - **Remnant quantities** determine the waveform's ringdown.

Conclusions

- **High dimensionality** of Precessing Systems → NR informed models are challenging.
  - Not enough NR Simulations to densely **cover** the 7-dim parameter space.
  - High q Simulations are computationally **expensive**: no NR information for $q > 18$.
  - The Emri Limit has to be used to **reduce the number** of NR simulations needed.
- We Created a **consistent and heterogeneous dataset** for quasi-circular precessing binaries, combining NR waveforms, NRSur7dq4 and the EMRI limit.
- We Generated fits for the **remnant properties** for the single spin across the η-dimension more accurate than `PhenXP` and faster than `NRSur7dq4`.
  - **Remnant quantities** determine the waveform's ringdown.
  - **Final spin morphology** as in EMRI limit: mix of linear and quadratic term in $1/q$.

CONCLUSIONS

- **High dimensionality** of PRECESSING SYSTEMS → NR informed models are challenging.
  - NOT ENOUGH NR SIMULATIONS to densely **cover** the 7-dim parameter space.
  - HIGH q SIMULATIONS are computationally **expensive**: no NR information for $q > 18$.
  - The EMRI LIMIT has to be used to **reduce the number** of NR simulations needed.
- We CREATED a **consistent and heterogeneous dataset** for quasi-circular precessing binaries, combining NR waveforms, NRSur7dq4 and the EMRI limit.
- We GENERATED fits for the **remnant properties** for the single spin across the η-dimension more accurate than `PhenXP` and faster than `NRSur7dq4`.
  - **Remnant quantities** determine the waveform's ringdown.
  - **Final spin morphology** as in EMRI limit: mix of linear and quadratic term in $1/q$.
  - **Single spin limit** as baseline for **double spin case**.

Acknowledgements

Maria de Lluc Planas is supported by the Spanish Ministry of Universities via an FPU doctoral grant (FPU20/05577). This work was supported by the Universitat de les Illes Balears (UIB); the Spanish Ministry of Science and Innovation (MCIN) and the Spanish Agencia Estatal de Investigación (AEI) grants PID2019-106416GB-I00/MCIN/AEI/10.13039/501100011033, RED2022-134204-E, RED2022-134411-T; the MCIN with funding from the European Union NextGenerationEU (PRTR-C17.I1); the FEDER Operational Program 2021-2027 of the Balearic Islands; the Comunitat Autònoma de les Illes Balears through the Direcció General de Política Universitaria i Recerca with funds from the Tourist Stay Tax Law ITS 2017-006 (PRD2018/23, PDR2020/11); the Conselleria de Fons Europeus, Universitat i Cultura del Govern de les Illes Balears; and EU COST Actions CA18108 and CA17137. We thank Scott A. Hughes, Anuj Apte, Gaurav Khanna and Halston Lim for providing the EMRI waveforms used in this project. I also extend my sincere appreciation to the CAPRA organising committee, the EDI team and the NBI for their financial support, enabling me to participate in this meeting.

Plan de Recuperación, Transformación y Resiliencia

Universitat de les Illes Balears

una manera de fer europa

Illes Balears Sostenibles

IAC3 Institute of Applied Computing & Community Code.

Unión Europea

GOVERN ILLES BALEARS

GOBIERNO DE ESPAÑA MINISTERIO DE CIENCIA E INNOVACIÓN

AGENCIA ESTATAL DE INVESTIGACIÓN

GOBIERNO DE ESPAÑA MINISTERIO DE UNIVERSIDADES